Assignment of the Absolute Configuration of β-Chiral Primary Alcohols by NMR: Scope and Limitations

Shamil K. Latypov,† María J. Ferreiro, Emilio Quiñoá, and Ricardo Riguera*

Contribution from the Departamento de Química Orgánica, Facultad de Química, and the Instituto de Acuicultura, Universidad de Santiago de Compostela, 15706 Santiago de Compostela, Spain

Received July 28, 1997

Abstract: The prediction of the absolute configuration of β-chiral primary alcohols from the ^{1}H NMR spectra of their esters with (*R*)- and (*S*)-9-anthrylmethoxyacetic acids (9-AMA, **3**) is discussed. Low-temperature NMR experiments, MM, semiempirical, ab initio, and aromatic shielding effect calculations allowed the identification of the main conformers and showed that, in all alcohols for which the calculated ΔE^{ag} (CVff) is in the range of 0.7−1.5 kcal/mol, conformer ***a/a*** is the most stable. A simple model for the assignment of the absolute configuration from NMR data is presented and its reliability corroborated with alcohols (**8**−**20**) of known configuration. Nevertheless, cyclic alcohols **21**−**23** have much higher ΔE^{ag} values (2.2−3.1 kcal/mol) due to their different conformational composition, and their absolute configuration cannot be reliably predicted by this method.

Introduction

The determination of the absolute configuration of organic compounds by NMR constitutes a research area of increasing interest due to the general availability of the instruments, the small amount of sample needed, and the simplicity of the method. Although many papers have been published on this topic, so far only two classes of substrate and one type of auxiliary reagent have been fully investigated.[1] The former are secondary alcohols and primary amines with the asymmetric center at the α-carbon, and the latter are arylmethoxyacetic acids (AMAAs).[2] The method is based on the derivatization of the alcohol or amine with the (*R*)- and (*S*)-enantiomers of the AMAA reagent followed by the comparison of the ^{1}H NMR spectra of the resulting diastereomers. The chemical shifts of the L_1/L_2 substituents at the asymmetric center of the substrate in the (*R*)- and (*S*)-derivatives reflect the influence of the aryl ring, and therefore, a correlation can be established between the spatial position of the aryl ring (known absolute configuration of the auxiliary reagent) and the position of the L_1/L_2 substituents of the substrate (unknown absolute configuration) (Figure 1).

This methodology has been fully supported by extensive conformational analysis and comparison of experimental and calculated shielding effects[3] and substantiated by examination of a large number of substrates of known stereochemistry. These studies have also indicated that the difference in chemical shifts observed for L_1/L_2 in the (*R*)-and (*S*)-AMAA derivatives (measured as $\Delta\delta^{RS}$)[4] is determined by the strength of the aromatic shielding effect and by the conformational composition (structure and relative abundance of the conformers). The merits and limitations of the classical MPA (**1**) and MTPA (**2**) reagents[5] (see Chart 1) and the advantages of new and more efficient reagents such as 9-AMA (**3**) have been discussed.[2c,3] Simple models that are useful to predict the absolute configuration of secondary alcohols and amines by NMR have been developed.[2]

It would be beneficial to extend the use of this methodology to other functional groups. Primary alcohols are interesting candidates for such studies because they are frequently found in nature in chiral form. If a correlation between the NMR properties of appropiate derivatives and stereochemistry were found, the assignment of the absolute configuration (and that

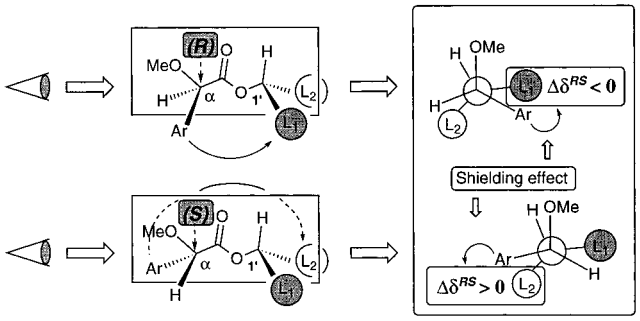

Figure 1. Selective influence of the aryl ring on both sides of the secondary alcohol moiety depending on the absolute configuration of the AMAA.

* To whom correspondence should be addressed.

† Present address: The Institute of Organic and Physical Chemistry of The Russian Academy of Sciences, Kazan, 4200.1383, Tatarstan, Russian Federation.

(1) For a review on the use of NMR for assignment of absolute configuration and ee measurements see: Uray, G. *Houben-Weyl: Methods in Organic Chemistry*; Helchen, G., Hoffmann, R. W., Mulzer, J., Schaumann, E., Eds.; Thieme: Stuttgart, New York, 1996; Vol. 1, p 253.

(2) (a) Trost, B. M.; O'Krongly, D.; Belletire, J. L. *J. Am. Chem. Soc.* **1980**, *102*, 7595−7596. (b) Trost, B. M.; Bunt, R. C.; Pulley, Sh. R. *J. Org. Chem.* **1994**, *59*, 4202−4205. (c) Seco, J. M.; Latypov, Sh. K.; Quiñoá, E.; Riguera, R. *Tetrahedron Lett.* **1994**, *35*, 2921−2924. (d) Latypov, Sh. K.; Seco, J. M.; Quiñoá, E.; Riguera, R. *J. Org. Chem.* **1995**, *60*, 1538−1545. (e) Seco, J. M.; Latypov, Sh. K.; Quiñoá, E.; Riguera, R. *Tetrahedron: Asymmetry* **1995**, *6*, 107−110. (f) Kouda, K.; Kusumi, T.; Ping, X.; Kan, Y.; Hashimoto, T.; Asakawa, Y. *Tetrahedron Lett.* **1996**, *37*, 4541−4544.

(3) (a) Latypov, Sh. K.; Seco, J. M.; Quiñoá, E.; Riguera, R. *J. Org. Chem.* **1995**, *60*, 504−515. (b) Seco, J. M.; Latypov, Sh. K.; Quiñoá, E.; Riguera, R. *Tetrahedron* **1997**, *53*, 8541−8564.

(4) $\Delta\delta^{RS}$ represents the difference between the chemical shift of the same group of the alcohol in the (*R*)- and (*S*)-derivatives ($\Delta\delta^{RS} = \delta R - \delta S$).

(5) Latypov, Sh. K.; Seco, J. M.; Quiñoá, E.; Riguera, R. *J. Org. Chem.* **1996**, *61*, 8569−8577.

S0002-7863(97)02550-X CCC: $15.00
Published on Web 05/02/1998

Chart 1

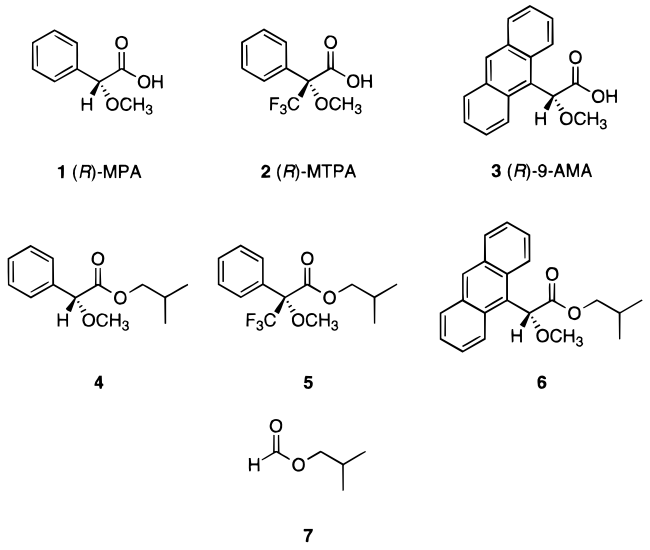

of potential precursors, such as carboxylic acids and aldehydes) would be easily attained.

However, a number of intrinsic difficulties can be seen due to the nature of primary alcohols: (1) The asymmetric center is, at best, at beta (β) or gamma (γ) positions with regard to the OH group. (2) The distance between groups L_1/L_2 of the substrate and the aryl ring of the auxiliary reagent is obviously larger than in secondary alcohols, and in addition, the longer chain between the chiral center and the auxiliary reagent should reduce the conformational preference. As a result, the $\Delta\delta^{RS}$ values in primary alcohols would be smaller and less reliable than those usually obtained from secondary alcohols.

The low conformational preference found in the esters of secondary alcohols,[5] together with the unfavorable orientation of the phenyl ring when facing L_1/L_2, suggests that neither MPA (**1**) or MTPA (**2**) would be good reagents for this purpose.

We have recently established[3] that the conformational equilibrium around the CO−C_α bond is strongly dependent on the nature of the aryl ring. Ab initio calculations and DNMR experiments on the 9-AMA (**3**) ester of a secondary alcohol have shown that (a) there is a strong conformational preference for the synperiplanar conformer (***sp***)[6] and (b) that the anthryl ring is oriented in such a way that L_1/L_2 remain well within the aromatic magnetic cone (maximum shielding zone). Therefore, we may reasonably expect a reduction in the flexibility of the ester and a greater efficiency in the transformation of the aromatic shielding into high-field shifts when using 9-AMA.

To test this supposition we studied the ^{1}H NMR spectra of the MPA, MTPA, and 9-AMA esters of 2-methylpropan-1-ol (compounds **4**−**6**, respectively), where the diastereotopic methyl groups are the L_1/L_2 substituents, and assessed the ability of each reagent to separate the L_1/L_2 signals. In fact, it was only in the case of ester **6** that completely separated signals were found ($\Delta\delta = 0.033$). Ester **4** showed only a slight separation (overlapped doublets, $\Delta\delta = 0.002$), while no noticeable discrimination was detected in ester **5**.

In this paper we describe our results on the assignment of the absolute configuration of primary alcohols with the asymmetric center at the β position by ^{1}H NMR spectroscopy of the corresponding (*R/S*)-9-AMA esters. A preliminary account has recently been published.[7]

(6) The ***sp*** conformer is defined by the synperiplanar conformation of the C_α-OMe and C═O groups.

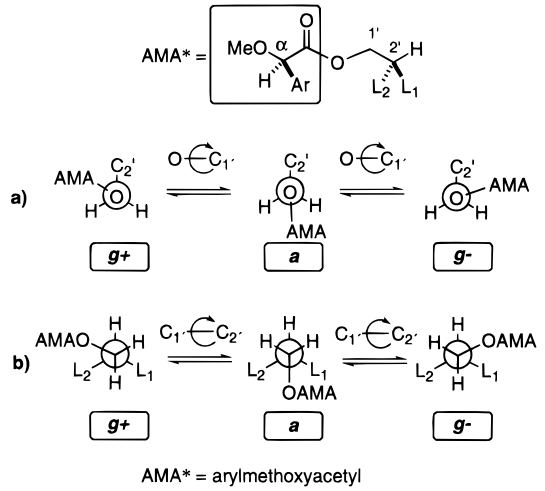

Figure 2. Main rotamers in the alcohol moiety of an AMA ester of a β-chiral primary alcohol by rotation around (a) the O−$C_{1'}$ and (b) the $C_{1'}$−$C_{2'}$ bonds.

Conformational Analysis of AMAA Esters of Primary Alcohols and the Aromatic Shielding Effect

The NMR parameters of flexible molecules depend on the structure and relative population of the main conformers. Therefore, in the case of the AMAA esters of a primary alcohol with a chiral carbon at the β position ($C_{2'}$), we have to analyze the rotation around the C_α−CO, CO−O, O−$C_{1'}$, and $C_{1'}$−$C_{2'}$ bonds. To keep this study within practical limits, we simplified this situation by considering the rotational mobility around the C_α−CO and CO−O bonds to be very low and considered those skeletal fragments to be almost rigid (Figure 2). Experimental data supporting restricted rotation around the CO−O bond has been provided by DNMR[8] and complemented by aromatic shielding calculations and ab initio data.[9] Similarly, the existence of a preferred ***sp*** rotamer around the C_α−CO bond in the 9-anthryl derivative is well documented.[3]

The remaining two bonds (O−$C_{1'}$ and $C_{1'}$−$C_{2'}$) are very flexible. Each bond can give rise to three low-energy rotamers (two gauche and one anti, Figure 3), and therefore the overall number of main rotamers that can be expected is 9. To study the behavior of this skeletal fragment in depth, isobutyl formate (**7**) was selected as the simplest model to perform molecular mechanics calculations (CVff). The results are presented in Figures 3 and 4.

Figure 3 shows the structures of the nine main conformers obtained by rotation around the O−$C_{1'}$ (vertical axis) and the $C_{1'}$−$C_{2'}$ bonds (horizontal axis). The corresponding energy map is presented in Figure 4. It shows that the rotamers that have the $C_{2'}$−$C_{1'}$−O−C(O)−H bonds in the same plane (***g***+/***a***, ***a***/***a***, and ***g***−/***a***, middle row, Figure 3) are the most stable ones and, therefore, those obtained by rotation around the O−$C_{1'}$ bond (columns) do not need to be considered. A similar precedent was previously observed in secondary alcohols, where rotation around the $C_{1'}$−O bond leads to a preferred gauche relationship between the $C_{1'}$−H and the O−C(O) bonds.[3]

(7) Ferreiro, M. J.; Latypov, Sh. K.; Quiñoá, E.; Riguera, R. *Tetrahedron: Asymmetry* **1996**, *7*, 2195−2198.

(8) (a) Drakenberg, T.; Forsen, S. *J. Phys. Chem.* **1972**, *76*, 3582−3586. (b) Grindley, T. B. *Tetrahedron Lett.* **1982**, *23*, 1757−1760.

(9) (a) Ohtani, I.; Kusumi, T.; Kashman, Yo.; Kakisawa, H. *J. Am. Chem. Soc.* **1991**, *113*, 4092−4096. (b) Tucker, J. A.; Houk, K. N.; Trost, B. M. *J. Am. Chem. Soc.* **1990**, *112*, 5465−5471.

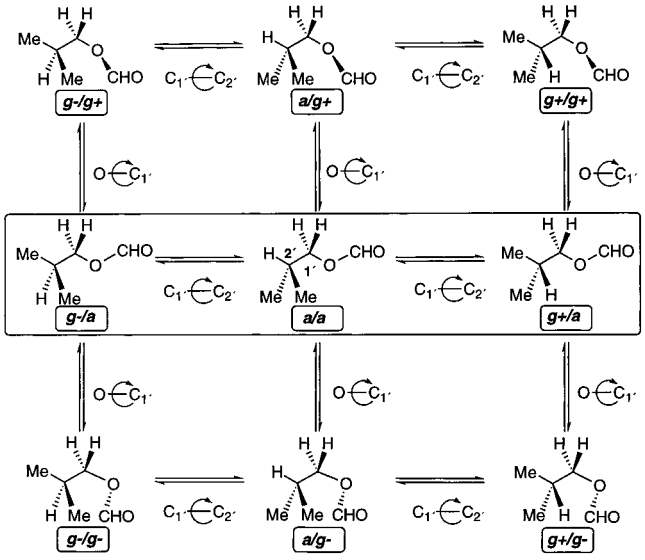

Figure 3. Low-energy conformers of isobutyl formate (**7**) as calculated by MM. The squares under each drawing contain two symbols that identify each conformer. The symbol on the left side defines the $C_{1'}-C_{2'}$ bond: ***a*** means $C_{2'}$−H anti to O−$C_{1'}$; ***g***+ or ***g***− means a 120° turn (clockwise or counterclockwise, respectively) from the ***a*** position. The symbol on the right side defines the O−$C_{1'}$ bond: ***a*** means $C_{1'}-C_{2'}$ *anti* to O−CHO; ***g***+ or ***g***− means a 120° turn (clockwise or counterclockwise, respectively) from the ***a*** position.

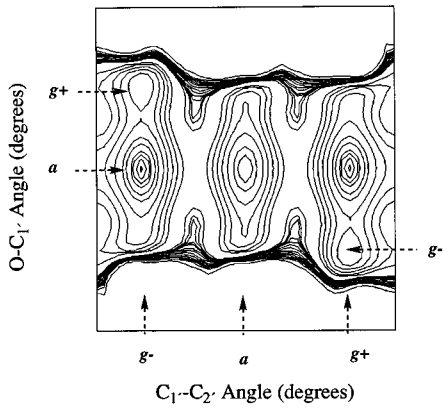

Figure 4. Energy contour map of ester **7** calculated by MM as a function of the dihedral angles around the O−$C_{1'}$ and $C_{1'}-C_{2'}$ bonds.

Experimental evidence of this conclusion was obtained by low-temperature NMR. We observed that at lower temperatures the NMR spectra of **7** showed the signals due to the protons at $C_{1'}$ shifted to higher field than at room temperature (3.875 ppm at 300 K and 3.847 ppm at 193 K) as a result of the shielding generated by the carbonyl group. This observation is in good agreement with an increase in the relative populations of conformers ***g***−/***a***, ***a***/***a***, and ***g***+/***a***,[10] and these should therefore be the most stable ones.

As for the $C_{1'}-C_{2'}$ bond, Figure 4 shows that no clear preference is found in the equilibrium around the $C_{1'}-C_{2'}$ bond, around which interconversion between the ***g***−/***a***, ***a***/***a***, and ***g***+/***a*** conformers occurs (middle row in Figure 3). The MM derived energy map suggests that rotamers ***g***−/***a*** and ***g***+/***a*** are a little more stable than rotamer ***a***/***a***. AM1 semiempirical calculations reiterate those results (Table 1), and therefore, we may conclude that the gauche ***g***+/***a*** and ***g***−/***a*** forms are the preferred ones. This preference seems reasonable when steric considerations between the substituents at $C_{2'}$ and the oxygen atom are considered (the methyl groups in **7** should destabilize the anti ***a***/***a*** form). However, other studies, including statistical mechanical Monte Carlo simulations, have indicated that the anti form (***a***/***a***) should be more stable than the gauche ones.[11] To assess the extent of this discrepancy and its consequences, we decided to check the accuracy of our MM and AM1 predictions by carrying out the energy calculations at a higher level.

Table 1. Comparison of Semiempirical and Nonempirical Data (in kcal/mol) for the Main Conformers of Compound **7**

conformer	MM (CVff)[12]	AM1[13]	ab initio[a]
gauche (***g***−/***a***, ***g***+/***a***)	0.00	0.00	0.10
anti (***a***/***a***)	0.87	0.87	0.00

[a] RHF/3-21G//RHF/3-21G.[14]

Table 2. Calculated Shielding Increments[a] for the Methyl Groups in the Main Conformers of 2-Methylpropan-1-ol 9-AMA Ester (**6**)

conformer	Me(1′)	Me(2′)
g+/***a***	ca. 0.14	ca. 0.55
a/***a***	ca. 0.82	ca. −0.05
g−/***a***	ca. −0.1	ca. 0.1

[a] Semiclassical model. See refs 3 and 21.

Table 1 shows the RHF/3-21G//RHF/3-21G ab initio calculations on ester **7**. These calculations show a slight preference for the anti as opposed to the gauche rotamers. This difference between the ab initio and the approximate methods can be ascribed to an underestimation of the stability of the anti form by MM and AM1 calculations of about 1 kcal/mol.

Once the existence of the three main conformations was established, the next goal was to estimate the participation of each conformer in the average NMR chemical shift. To this end, we carried out aromatic shielding effect calculations (semiclassical model) on the 9-AMA ester of 2-methylpropan-1-ol (**6**) following the previously established methodology.[3]

Table 2 shows the expected shielding on the methyl groups of **6** considering the conformers ***g***+/***a***, ***g***−/***a***, and ***a***/***a***. The results indicate that both methyl groups are subject to very different shielding in the ***g***+/***a*** and ***a***/***a*** conformers, while no appreciable difference is produced in conformer ***g***−/***a***. The greatest separation between Me(1′) and Me(2′) occurs in conformer ***a***/***a*** (0.82 vs −0.05), and this, therefore, becomes the most significant in terms of NMR spectroscopy. Conformer ***a***/***a*** is, in addition, the most populated one. Therefore, the average shielding is dominated by this conformer[15] and the relative chemical shifts of Me(1′) and Me(2′) can be effectively

(10) Balasubrahamanyam, S. N.; Bharathi, S. N.; Usga, G. *Org. Magn. Reson.* **1983**, *21*, 474−481.

(11) (a) Shimanouchi, T.; Ogawa, Y.; Ohta, M.; Matsuura, H.; Harada, I. *Bull. Chem. Soc. Jpn.* **1976**, *49*, 2990−3008. (b) Ogawa, Y.; Ohta, M.; Sakakibaba, M.; Matsuura, H.; Harada, I.; Shimanouchi, T. *Bull. Chem. Soc. Jpn.* **1977**, *50*, 650−660. (c) Andersson, M.; Karlstrom, G. *J. Phys. Chem.* **1985**, *89*, 4957−4962. (d) Hoppilliard, Y.; Solgadi, D. *Tetrahedron* **1980**, *36*, 377−380.

(12) Roberts, V. A.; Osguthorpe, D. I.; Wolff, J.; Genest, M.; Hagler, A. T. *Proteins: Struct., Funct., Genet.* **1988**, *4*, 31.

(13) (a) Dewar, M. J. S.; Zoebisch, E. G.; Healy, E. F.; Stewart, J. J. P. *J. Am. Chem. Soc.* ***1985***, *107*, 3902−3909. (b) Havel, T. F. *Prog. Biophys. Mol. Biol.* ***1991***, *56*, 43−78. (c) Stewart, J. J. P. *J. Comput. Chem.* **1989**, *10*, 209−220. (d) Komorinski, A.; McIver, W., Jr. *J. Am. Chem. Soc.* **1973**, *95*, 4512−4517.

(14) Frisch, M. J.; Trucks, G. W.; Head-Gordon, M.; Gill, P. M. W.; Wrong, M. W.; Foresman, J. B.; Johnson, B. G.; Schhlegel, H. B.; Robb, M. A.; Replogle, E. S.; Gomperts, R.; Andres, J. L.; Raghavachari, K.; Binkley, J. S.; Gonzalez, C.; Martin, R. L.; Fox, D. J.; Defrees, D. J.; Baker, J.; Stewart, J. J. P.; Pople, J. A. *GAUSSIAN 92*, revision D.1; Gaussian: Pittsburgh, PA, 1992.

(15) Inspection of the aromatic shielding effects values shown in Table 2 indicates that conformer ***a***/***a*** would be the NMR significant one even if the three conformers were equally populated.

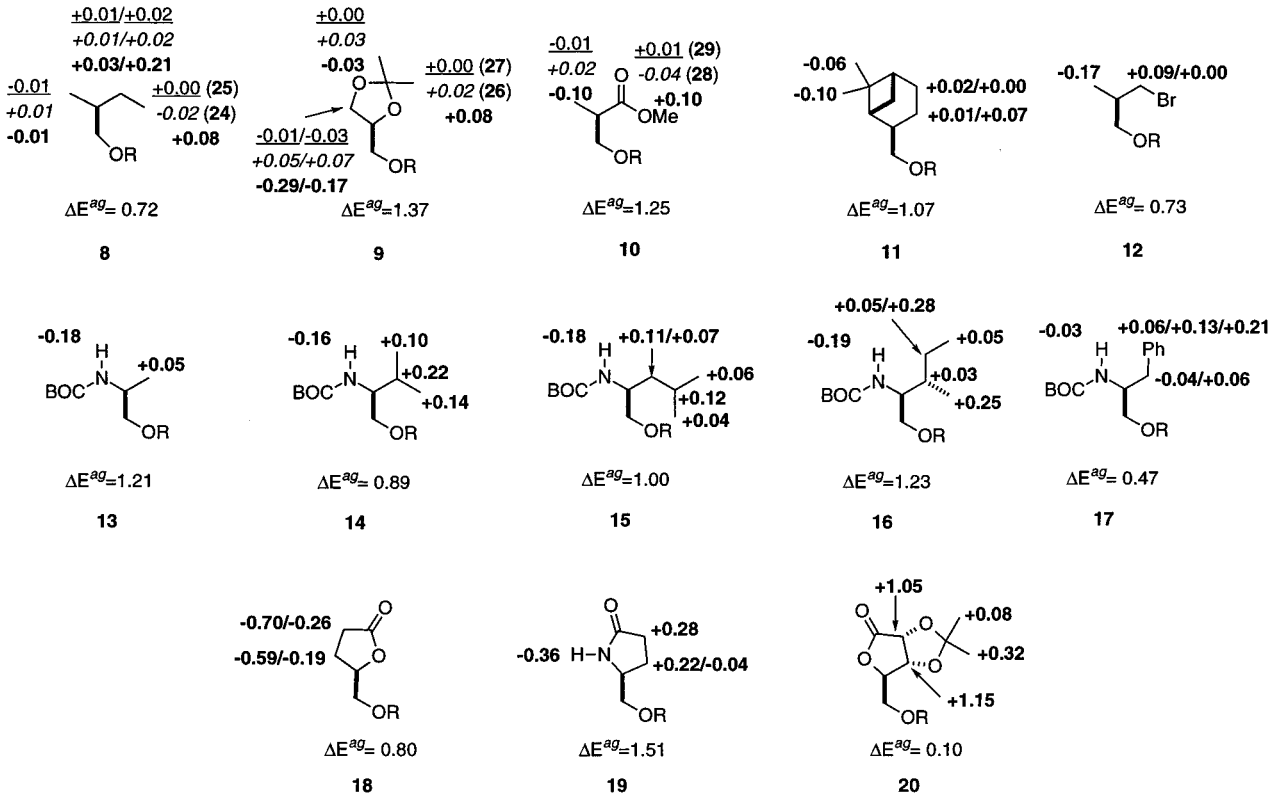

Figure 5. ΔE^{ag} (CVff, in kcal/mol) and $\Delta\delta^{RS}$ values for the 9-AMA esters of compounds **8**−**20**. Selected $\Delta\delta^{RS}$ values for some MPA (compounds **24**, **26**, and **28**) and MTPA (compounds **25**, **27**, and **29**) esters are also shown.

predicted from their position relative to the aryl group in conformer ***a*/*a*** [i.e. Me(1′) is shielded in the (*R*)-ester and Me(2′) is shielded in the (*S*)-ester].

To see if the above conclusions on model compound **6** can be applied generally to allow the establishment of a secure and reliable NMR connection between the absolute configuration at the asymmetric center of the auxiliary reagent and that of the alcohol, we carried out MM calculations (CVff) on primary alcohols **8**−**23**, of known absolute configuration. Their structures are shown in Figures 5 and 6 along with the calculated energy difference between the gauche and anti forms ($\Delta E^{ag} = E^a - E^g$).

Compounds **8**−**20** (Figure 5) show ΔE^{ag} values in the range 0.72−1.51 kcal/mol. These are close to the calculated values for model **6** and should clearly also be affected by the underestimation of the stability of the anti form associated with the MM method. Nevertheless, the preference for the ***a*/*a*** form shown by ab initio calculations can be easily restored in all cases by the introduction of a correction factor of −1.4 kcal/mol (to be added to the CVff value). In contrast, MM calculations on compounds **21**−**23** (Figure 6) produce much higher ΔE^{ag} values (2.20−3.08 kcal/mol) due to excessive destabilization of the ***a*/*a*** form, which in **21**−**23** is no longer the preferred one, with ***g*−/*a*** and ***g*+/*a*** forms now making a very significant contribution.

The above results clearly indicate that, among all the primary alcohols studied, two different groups can be distinguished: compounds **8**−**20**, which are conformationally similar to model **6** and have $\Delta E^{ag} = 0.72-1.51$, and compounds **21**−**23**, which behave in a different way and show much higher ΔE^{ag} values (2.20−3.08).

NMR Results

Experimental evidence confirming that the ***a*/*a*** form is both the most populated and NMR significant one in compounds **8**−**20** was obtained from the low-temperature ^{1}H NMR spectra of the (*R*)- and (*S*)-9-AMA esters of (*S*)-(−)-2-methylbutan-1-ol (**8**). For instance, Me(4′) in the (*S*)-9-AMA ester and Me(5′) in the (*R*)-9-AMA ester show upfield shifts (by 0.038 and 0.008 ppm, respectively) at low temperature (183 K), relative to the signals at room temperature, in agreement with their position under the shielding cone of the anthryl ring in the ***a*/*a*** form, but they shift to lower field [by 0.047 ppm for Me(4′) in the (*R*)- and 0.103 ppm for Me(5′) in the (*S*)-ester] when they are located in the nonshielding cone area.

A crude evaluation of the experimental shielding increments suffered by Me(4′) in **8**, for example, can be obtained as the difference between its chemical shift in the 9-AMA esters and in the free alcohol **8**, [ca. 0.392 ppm in the (*R*)-9-AMA and 0.359 ppm in the (*S*)-9-AMA]. Comparison with the calculated values for conformer ***a*/*a*** in model compound **6** (ca. 0.82 ppm, Table 2) points to the aromatic shielding effect of the anthryl group as being responsible for the observed high-field shift and confirms 9-AMA to be a very efficient shielding reagent. In addition, this comparison suggests that the conformer that produces shielding amounts to ca. 44−48% of the population in the 9-AMA ester. In terms of energy, this corresponds to a preference for the ***a*/*a*** form of about 0.27−0.37 kcal/mol at 183 K, a value which is in good general agreement with the results of ab initio calculations.

Comparison of the NMR spectra of **8** and its esters with both enantiomers of 9-AMA, MPA, and MTPA (Figure 7) illustrates these results very well: while in the MPA and MTPA derivatives, Me(4′) and Me(5′) resonate at virtually the same chemical shift as in the free alcohol, in the 9-AMA ester the

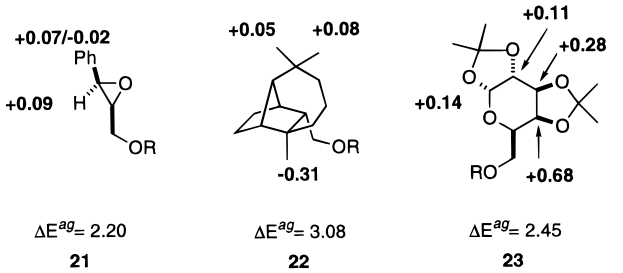

Figure 6. ΔE^{ag} (CVff, in kcal/mol) and $\Delta\delta^{RS}$ values for the 9-AMA esters of compounds **21**−**23**.

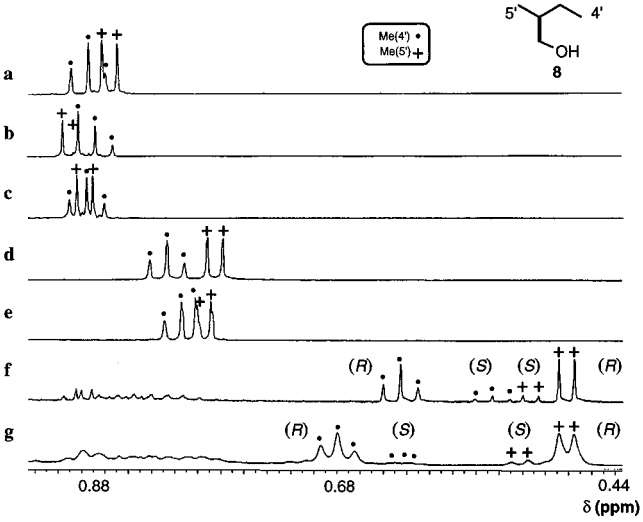

Figure 7. Partial ^{1}H NMR spectra (3:1 CS_2−CD_2Cl_2) of (a) 2-methylbutan-1-ol (**8**); (b) (*R*)-MTPA ester; (c) (*S*)-MTPA ester; (d) (*R*)-MPA ester; (e) (*S*)-MPA ester; (*R*)-9-AMA and (*S*)-9-AMA esters (88:12) (f) at room temperature and (g) at 183 K.

shielding produced by the anthryl ring effectively shifts Me(4′) and Me(5′) upfield by $\Delta\delta = 0.25-0.40$ in relation to the free alcohol. Analogous results were obtained when the comparison was extended to alcohols **9** and **10** (Figure 5), confirming that 9-AMA (**3**) is a good reagent for producing shielding for primary alcohols. However, no useful $\Delta\delta^{RS}$ values or a general trend in the signs was observed when MPA (**1**) and MTPA (**2**) were used as derivatizing agents, as shown in Figure 5 for derivatives **24**−**29**.

Model for the Determination of the Absolute Configuration of β-Chiral Primary Alcohols from the ^{1}H NMR of Their 9-AMA Esters

All the information presented to this point strongly suggests that a correlation exists between the spatial location of the anthryl ring at the asymmetric center of the reagent and that of substituents L_1/L_2 around the asymmetric center of the alcohol and, therefore, that the absolute configuration at the asymmetric center of the acid (C_α) can be correlated to that of the alcohol ($C_{2'}$) by NMR.

Experimental evidence was obtained from the ^{1}H NMR spectra of the alcohols of known absolute configuration shown in Figure 5. The $\Delta\delta^{RS}$ values obtained are sufficiently large (and well outside the experimental error) that they are of practical use, and their signs are homogeneously distributed in accordance with the spatial arrangement of the substituents in relation to the anthryl ring.

Figure 8 illustrates the reasoning outlined above for compound **8**, showing the full accordance between the experimental NMR data and the low-energy conformers deduced from the calculations. The structures shown for the (*R*)- and (*S*)-9-AMA esters of **8** combine both the ***a***/***a*** conformer of the alcohol moiety (discussed in this work) and the most stable ***sp*** conformer previously deduced for the acid substructure.[3,5] For instance, Me(5′) lies on the same side as the aryl ring in the (*R*)- ester and, therefore, its signal is shifted to higher field than that in the (*S*)-ester (negative $\Delta\delta^{RS}$). The opposite is observed for the ethyl substituent [i.e. Me(4′)], which is closer to the aryl ring in the (*S*)-ester (positive $\Delta\delta^{RS}$). As a conclusion, and in accordance with the ***a***/***a*** and ***sp*** conformers, the absolute configuration of **8** must be (*S*).

This correlation between the signs of $\Delta\delta^{RS}$ and the absolute configuration of the alcohol works well in all the compounds shown in Figure 5. The sign of $\Delta\delta^{RS}$ is consistently positive or negative for all protons located on a certain side of the asymmetric center and indicates that the absolute configuration of these primary alcohols can be determined by interpretation of the chemical shifts of L_1/L_2 in the (*R*)- and (*S*)-9-AMA esters in the light of the conformational model shown in Figure 9, where the MeO−C_α−CO−O−$C_{1'}$−$C_{2'}$−H bonds are in the same plane.

In this way, identification of substituent L_1 as the one that resonates at higher field in the (*R*)-9-AMA ester than in the (*S*)-ester (negative $\Delta\delta^{RS}$; Figure 9) and of L_2 as the substituent that resonates at higher field in the (*S*)- than in the (*R*)-ester (positive $\Delta\delta^{RS}$) allows the spatial location of L_1 and L_2 around $C_{2'}$ to be established and makes the assignment of the absolute configuration a simple task.

However, the NMR spectra of compounds **21**−**23** show that they do not conform to the model discussed above, and their high preference for gauche forms leads to signs of $\Delta\delta^{RS}$ which are in disagreement with the above reasoning. Indeed, it must be stressed that the configuration deduced in this way is not reliable.

Scope and Limitations

Inspection of the structures of compounds **8**−**20** indicates that the model shown in Figure 9 can be applied to a wide variety of β-chiral primary alcohols with a diverse range of functions and substitution patterns and that the presence of polar groups does not adversely affect its reliability. At the same time, we have reported that it cannot be used with compounds **21**−**23** because of their different conformational composition.

It is very important to point out that the model has worked correctly for all the alcohols in which the chiral center was not part of (i.e. **8**, **10**, **12**, **13**−**17**) and in most cases in which it is part of a cyclic system (i.e. **9**, **11**, **18**−**20**).

Clearly, it is imperative to define clear criteria to distinguish those primary alcohols whose stereochemistry can be investigated by this method and those that are not suitable due to their different conformational composition. This could surely be performed by ab initio calculations (Table 1), but these are time-consuming and simpler methods would be certainly cheaper.

MM is an alternative which could be considered. It is fast, and the ΔE^{ag} values obtained for **8**−**20** are coherent within the whole series and are significantly different from those obtained for **21**−**23**. These facts make it a suitable method to be used to distinguish between the two groups of compounds. Unfortunately, the CV force field produces a systematic excess of gauche over anti conformers that has to be corrected by about −1.4 kcal/mol to restore the preference (anti forms are more stable than gauche forms by about 0.3 kcal/mol) indicated by ab initio and NMR results obtained on **8**−**20**.

To see if other force fields would be more advantageous, we carried out MM calculations on compounds **6**−**23** with other

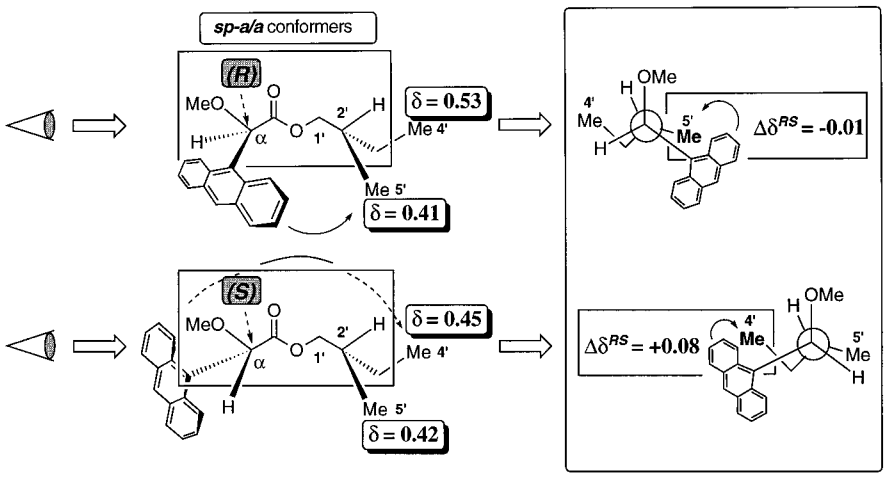

Figure 8. Low-energy conformers of the 9-AMA esters of **8** with selected NMR data.

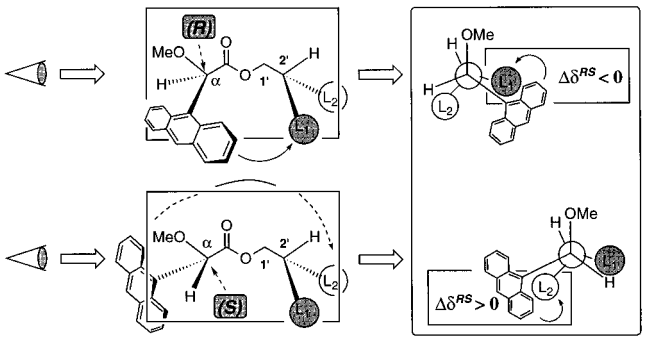

Figure 9. Conformational model for the determination of the absolute configuration of β-chiral primary alcohols by NMR spectroscopy.

options.[16] The data contained in Table 3 show PCff91[17] as the method that best reproduces the existence of two groups of compounds (set **6**−**20**, where the ***a***/***a*** conformer is more stable than the gauche conformers, and set **21**−**23**, in which the behavior is the other way round) and give the ΔE^{ag} values closest to the real ones (ab initio and NMR).

The force fields Amber[18] and CVff[12] produce overstabilization of the gauche forms; nevertheless, the ΔE^{ag} values obtained allow a distinction to be made between set **6**−**20** [small stabilization of gauche, ΔE^{ag}= 0.5−2.3 (Amber), 0.7−1.4 (CVff)] and set **21**−**23**, where the overstabilization is very large [ΔE^{ag}= 3.8 (Amber), 2.2−3.1 (CVff)].

Finally, MMX[19] calculations give results similar to Amber and CVff, but the parametrization is not good enough to adequately reproduce all the structural features of **6**−**23**, and some energy values are out of range.

Conclusions

In conclusion, the absolute configuration of almost all β-chiral primary alcohols can be safely assigned by ^{1}H NMR spectroscopy of the (*R*)- and (*S*)-9-AMA esters, employing the model shown in Figure 9. If the chiral center is part of a ring, or when strong steric interactions could be in operation, ab initio or MM calculations must be performed in order to ensure that the anti form is the most stable one. All the force fields used in MM calculations show the difference between the two types of compounds, but PCff is the best and it can be safely used as an alternative to ab initio calculations to predict the suitability of a primary alcohol for this method. Greater values than those observed for compounds **6**−**20** are an indication of a different conformational composition and, therefore, that the assignment of the absolute configuration will be unreliable.

Experimental Section

Computational Methods. Molecular mechanics (employing the PC91 force field[17]) and AM1 (PM3) calculations were performed using the Insight II package on a Silicon Graphics Iris (SGI) computer. Initial molecular geometries were originated from the Builder Module of Insight II; 3D coordinates were then generated from the bond lengths, bond angles, and dihedral angles using the DG-II package.[20] The conformational space of each compound was scanned by MM optimization of the sterically allowed conformations around key single bonds. The MM simulations were carried out *in vacuo*. Analysis of conformational transitions, identification of the low-energy conformers, and calculation of the energy barriers between these conformers were all carried out by MM. The energies of conformations were minimized in Cartesian coordinate space by the block diagonal Newton−Raphson method; minima corresponded to rms energy gradients < 0.001 kcal/(mol Å). The ground-state energies of the geometries were then calculated by AM1 (PM3) using the MOPAC 6.0 program. For all compounds, full geometry optimization used the Broyden−Fletcher−Goldfarb−Shanno (BFGS) method and the PRECISE option.[13] Ab initio electronic structure calculations (at the restricted Hartree−Fock level of theory) were performed using GAUSSIAN 92.[14] During the ab initio calculations all internal coordinates were optimized by Berny algorithm and convergence was tested against criteria for the maximum force component, root-mean-square force, maximum step component, and root-mean-square step. No symmetry options were implemented.

Shielding effects calculations based on the semiclassical model of Bovey and Johnson[21] were carried out using an SGI computer. No corrections for local anisotropic contributions[21d,e] were implemented. Calculations were performed with π-current loops separation of 1.39 Å.[21b,f]

NMR Spectroscopy. ^{1}H and ^{13}C NMR spectra of samples in 4:1 CS_2/CD_2Cl_2 or $CDCl_3$ (ca. 2−3 mg in 0.5 mL) were recorded on a AMX 500, AMX 300, or WM 250 NMR spectrometer. Chemical shifts (ppm) are internally referenced to the tetramethylsilane signal (0 ppm)

(16) For a recent comparative study see: Gundertofte, K.; Liljefors, T.; Norrby, P.; Ptterson, I. *J. Comput. Chem.* **1996**, *17*, 429−449.
(17) Maple, J. R.; Dinur, U.; Hagler, A. T. *Proc. Natl. Acad. Sci. U.S.A.* **1988**, *85*, 5350−5354.
(18) Kollman, P. A.; Weiner, S.; Seibel, G.; Lybrand, T.; Singh, U. Ch.; Caldwell, J.; Rao, Sh. N. *Ann. N. Y. Acad. Sci*. **1986**, *482*, 234−244.
(19) Gajewski, J. J.; Gilbert, K. E.; Mckelvey, J. *Adv. Mol. Model.* **1990**, *2*, 65−92.
(20) Cioslowski, J.; Kertesz, M. *QCPE Bull.* **1987**, *7*, 159.
(21) (a) Waugh, J. S.; Fessenden, R. W. *J. Am. Chem. Soc.* **1957**, *79*, 846−849. (b) Johnson. C. E.; Bovey, F. A. *J. Chem. Phys.* **1958**, *29*, 1012−1014. (c) Jonathan, N.; Gordon, S.; Dailey, B. P. *J. Chem. Phys.* **1962**, *36*, 2443−2448. (d) Dailey, B. P. *J. Chem. Phys.* **1964**, *41*, 2304−2310. (e) Musher, J. I. *J. Chem. Phys.* **1965**, *42*, 4081−4083. (f) Haigh, C. W.; Mallion, R. B. Ring current theories in NMR. *Progress in NMR spectroscopy*; Pergamon Press: London, 1980; Vol. 13, pp 303−344.

Table 3. Conformational Energy Distribution (in kcal/mol) around the $C_{1'}-C_{2'}$ Bond for Alcohols **7**−**23** Obtained in the Framework of Several Force Fields

	amber			CVff			PCff91			MMX[a]		
	a	***g*+**	***g*−**	***a***	***g*+**	***g*−**	***a***	***g*+**	***g*−**	***a***	***g*+**	***g*−**
7	0.54	0.00		0.87	0.00	0.00	0.00	0.39		0.64	0.00	
8	0.42	0.00	0.11	0.72	0.00	0.21	0.00	0.54	0.55	0.46	0.00	0.10
9	2.34	0.00	1.89	1.37	0.00	1.04	0.10	0.00	0.39	0.52	0.00	0.21
10	1.07	0.01	0.14	1.25	0.00	0.69	0.00	0.26	0.43	0.21	0.00	0.42
11	1.08	0.00	0.11	1.07	0.00	0.05	0.00	0.06	0.17	1.43	0.00	0.18
12	*b*	*b*	*b*	0.73	0.00	0.80	0.00	0.56	0.80	0.52	0.00	0.34
13	0.90	0.00	1.88	1.21	0.00	0.72	0.00	0.64	6.89	0.67	0.00	0.36
14	0.00	0.47	1.55	0.89	0.00	0.52	0.00	0.02	7.34	0.25	0.00	1.74
15	0.86	0.00	1.86	1.00	0.00	0.89	0.00	0.52	6.75	0.69	0.00	0.58
16	0.87	0.00	1.19	1.23	0.00	0.34	0.00	0.24	7.21	0.30	0.00	0.18
17	0.00	0.69	0.19	0.47	0.00	0.75	0.00	0.04	6.71	1.35	0.00	0.31
18	0.48	0.00	0.29	0.80	0.00	0.29	0.00	0.06	0.34	0.00	2.07	2.44
19	1.04	0.00	0.62	1.51	0.00	0.45	0.00	0.59	6.76	0.69	0.00	0.21
20	0.00	1.14	1.36	0.10	0.00	0.34	0.00	0.03	0.61	0.63	0.00	0.34
21	*c*	0.00	1.67	2.20	0.00	1.00	0.00[d]	0.55[d]	0.30[d]	1.58	0.00	0.33
22	3.82	0.00	0.22	3.08	0.00	0.10	2.71	0.00	0.40	4.83	0.00	0.24
23	*b*	*b*	*b*	2.45	0.00	0.98	0.96	0.00	0.79	2.40	0.00	1.95

[a] pc4.41. [b] The potential type cannot be assigned. [c] Unstable structure. [d] A full set of force fields is not available.

in all cases. One- and two-dimensional NMR spectra were measured with standard pulse sequences. 2D homo- (COSY) and heteronuclear (HMQC) shift correlation experiments were carried out using pulsed field gradient technique. Apodization with a shifted sine bell and baseline correction was implemented to process 2D spectra.

1D ^{1}H NMR Spectra. Size 32 K, pulse length 2.8 ms (30°), 16 acquisitions.

2D COSY Spectra. Sequence: D1−90−t_1−G_1−90−G_2−AQ; relaxation delay D1 = 1 s, 90° pulse 8.5 μs, gradient ratio 1:1.

2D TOCSY Spectra. Relaxation delay D1 = 2 s; mixing time 41.3 ms; 90° pulse 8.5 μs; TPPI-mode, NS = 64.

2D Proton-Detected Heteronuclear Multiple Quantum Correlation (HMQC) Experiments. Sequence: D190(^{1}H)−D2−90(^{13}C)−t_1/2−G1−180(^{1}H)−G2−t_1/2−90(^{13}C)−G3−D2−AQ (GARP(^{13}C)), relaxation delay D1 = 2s; D2 = 3.45 ms; 90° pulse (^{1}H) 8.5 μs; 90° pulse (^{13}C) 10.5 μs, gradient ratio 5:3:4.

For DNMR spectroscopy, the probe temperature was controlled by a standard unit calibrated using a methanol reference; samples were allowed to equilibrate for 15 min at each temperature before recording spectra.

General Methods. Preparation of diastereomeric esters **4**−**29** from the corresponding primary alcohols and (*R/S*)-9-anthrylmethoxyacetic acid (9-AMA) was carried out with DCC and DMAP.[22] Final purification was achieved by HPLC (μ-Porasil 3 mm × 250 mm or Spherisorb S5W 5 mm, hexanes−ethyl acetate). The *N*-BOC-amino alcohols were obtained from the corresponding Boc-protected amino acids by reduction with BH_3·THF at 0 °C.[23] Retention of configuration was observed in all cases.

2-Methylpropyl (*R*)-(−)-2-methoxy-2-phenylacetate ((*R*)-4): [α] = −79.0 (c = 0.012, $CHCl_3$); ^{1}H NMR (300.13 MHz, $CDCl_3$) δ (ppm) 0.81 (d, J = 6.7 Hz, 3H), 0.82 (d, J = 6.7 Hz, 3H), 1.87 (m, 1H), 3.41 (s, 3H), 3.90 (d, J = 6.8 Hz, 2H), 4.77 (s, 1H), 7.33 (m, 3H), 7.43 (m, 2H); UV λ_{max} 242 nm ($CHCl_3$); MS (EI) *m*/*z* 222 (M^+); HRMS (EI) $C_{13}H_{18}O_3$ found 222.11262, calcd 222.11256, Δm −0.06 mu.

2-Methylpropyl (*R*)-(−)-2-methoxy-2-(trifluoromethyl)-2-phenylacetate: ((*R*)-5): [α] = +11.6 (c = 0.005, $CHCl_3$); ^{1}H NMR (300.13 MHz, $CDCl_3$) δ (ppm) 0.93 (d, J = 6.7 Hz, 6H), 2.00 (m, 1H), 3.55 (s, 3H), 4.06 (dd, J = 6.5, 10.6 Hz, 1H), 4.15 (dd, J = 6.5, 10.6 Hz, 1H), 7.41 (m, 3H), 7.51 (m, 2H); UV λ_{max} 232 nm ($CHCl_3$); MS (EI) *m*/*z* 290 (M^+); HRMS (EI) $C_{14}H_{17}O_3F_3$ found 290.11300, calcd 290.11298, Δm −0.02 mu.

2-Methylpropyl (*R*)-(−)-2-(9-anthryl)-2-methoxyacetate ((*R*)-6): [α] = −23.2 (c = 0.033, $CHCl_3$); ^{1}H NMR (300.13 MHz, $CDCl_3$) δ (ppm) 0.51 (d, J = 6.7 Hz, 3H), 0.54 (d, J = 6.7 Hz, 3H), 1.62 (m, 1H), 3.43 (s, 3H), 3.82 (d, J = 6.7 Hz, 2H), 6.29 (s, 1H), 7.54 (m, 4H), 8.02 (d, J = 8.3 Hz, 2H), 8.48 (s, 1H), 8.58 (d, J = 8.9 Hz, 2H); UV λ_{max} 260 nm ($CHCl_3$); MS (EI) *m*/*z* 322 (M^+); HRMS (EI) $C_{21}H_{22}O_3$ found 322.15740, calcd 322.15690, Δm −0.50 mu.

(*S*)-(−)-2-Methylbutyl (*R*)-(−)-2-(9-anthryl)-2-methoxyacetate ((*R*)-8): HPLC t_R = 21.83 min (hexanes−ethyl acetate, 96:4, 2 mL/min, μ-porasil); [α] = −61.6 (c = 0.005, EtOH); ^{1}H NMR (500.13 MHz, $CDCl_3$) δ (ppm) 0.41 (d, J = 6.7 Hz, 3H), 0.53 (t, J = 7.6 Hz, 3H), 0.75 (m, 1H), 0.93 (m, 1H), 1.34 (m, 1H), 3.37 (s, 3H), 3.79 (dd, J = 6.8, 10.8 Hz, 1H), 3.86 (dd, J = 6.0, 10.8 Hz, 1H), 6.23 (s, 1H), 7.40 (dd, J = 6.8, 8.1 Hz, 2H), 7.47 (dd, J = 6.5, 7.9 Hz, 2H), 7.94 (d, J = 8.6 Hz, 2H), 8.39 (s, 1H), 8.53 (d, J = 8.9 Hz, 2H); ^{13}C NMR (75.47 MHz, $CDCl_3$) δ (ppm) 10.8, 15.8, 25.6, 33.7, 57.5, 69.6, 77.2, 124.5, 125.0, 126.4, 127.4, 129.1, 130.5, 131.4, 171.4; UV λ_{max} 260 nm ($CHCl_3$); MS (EI) *m*/*z* 336 (M^+); HRMS (EI) $C_{22}H_{24}O_3$ found 336.17293, calcd 336.17254, Δm −0.39 mu. Anal. Calcd for $C_{22}H_{24}O_3$: C, 78.53; H, 7.2. Found: C, 78.89; H, 7.12.

(*S*)-(−)-2-Methylbutyl (*S*)-(+)-2-(9-anthryl)-2-methoxyacetate ((*S*)-8): HPLC t_R = 23.11 min (hexanes−ethyl acetate, 96:4, 2 mL/min, μ-porasil); [α] = +154.4 (c = 0.0025, EtOH); ^{1}H NMR (500.13 MHz, $CDCl_3$) δ (ppm) 0.42 (d, J = 6.7 Hz, 3H), 0.45 (t, J = 7.4 Hz, 3H), 0.67 (m, 1H), 0.75 (m, 1H), 1.31 (m, 1H), 3.36 (s, 3H), 3.80 (d, J = 6.3 Hz, 2H), 6.21 (s, 1H), 7.40 (dd, J = 7.4, 8.3 Hz, 2H), 7.47 (dd, J = 6.4, 8.7 Hz, 2H), 7.94 (d, J = 8.6 Hz, 2H), 8.40 (s, 1H), 8.50 (d, J = 9.0 Hz, 2H); ^{13}C NMR (75.47 MHz, $CDCl_3$) δ (ppm) 10.8, 15.9, 25.5, 33.8, 57.5, 69.6, 77.2, 124.4, 125.0, 126.4, 127.4, 129.1, 130.5, 131.4, 171.4; UV λ_{max} 260 nm ($CHCl_3$); MS (EI) *m*/*z* 336 (M^+); HRMS (EI) $C_{22}H_{24}O_3$ found 336.17285, calcd 336.17254, Δm −0.31 mu.

D-α,β-Isopropylidenegliceryl (*R*)-(−)-2-(9-anthryl)-2-methoxyacetate ((*R*)-9): HPLC t_R = 27.53 min (hexanes−ethyl acetate, 80:20, 2 mL/min, Spherisorb S5W 5μm); [α] = −30.4 (c = 0.0025, EtOH); ^{1}H NMR (500.13 MHz, $CDCl_3$) δ (ppm) 0.94 (s, 3H), 1.09 (s, 3H), 2.91 (dd, J = 6.3, 8.4 Hz, 1H), 3.36 (dd, J = 6.3, 8.4 Hz, 1H), 3.37 (s, 3H), 3.90 (m, 1H), 3.98 (dd, J = 5.4, 11.5 Hz, 1H), 4.07 (dd, J = 4.2, 11.6 Hz, 1H), 6.23 (s, 1H), 7.40 (m, 2H), 7.47 (m, 2H), 7.95 (d, J = 8.6 Hz, 2H), 8.42 (s, 1H), 8.46 (d, J = 8.9 Hz, 2H); ^{13}C NMR (75.47 MHz, $CDCl_3$) δ (ppm) 25.3, 26.1, 57.5, 64.1, 65.5, 72.8, 77.2, 109.3, 124.2, 125.0, 126.7, 129.2, 129.4, 130.6, 131.5, 171.2; UV λ_{max} 260 nm ($CHCl_3$); MS (EI) *m*/*z* 380 (M^+); HRMS (EI) $C_{23}H_{24}O_5$ found 380.16202, calcd 380.16237, Δm 0.35 mu. Anal. Calcd for $C_{23}H_{24}O_5$: C, 72.60; H, 6.36. Found: C, 72.91; H, 6.18.

D-α,β-Isopropylidenegliceryl (*S*)-(+)-2-(9-anthryl)-2-methoxyacetate ((*S*)-9): HPLC t_R = 30.21 min (hexanes−ethyl acetate, 80:20, 2 mL/min, Spherisorb S5W 5μm); [α] = +28.7 (c = 0.0055, EtOH); ^{1}H NMR (500.13 MHz, $CDCl_3$) δ (ppm) 0.97 (s, 3H), 1.01 (s, 3H), 3.20 (dd, J = 5.7, 8.4 Hz, 1H), 3.35 (s, 3H), 3.53 (dd, J = 5.7, 8.3 Hz, 1H),

(22) Trost, B. M.; Belletire, J. L.; Godleski, S.; McDougal, P. G.; Balkovec, J. M. *J. Org. Chem.* **1986**, *51*, 2370−2374.

(23) Stanfield C. F.; Parker J. E.; Kanellis P. *J. Org. Chem.* **1981**, *46*, 4799−4800.

3.89 (m, 2H), 4.11 (m, 1H), 6.23 (s, 1H), 7.39 (m, 2H), 7.46 (m, 2H), 7.93 (d, J = 8.4 Hz, 2H), 8.40 (s, 1H), 8.47 (d, J = 9.0 Hz, 2H); ^{13}C NMR (62.97 MHz, $CDCl_3$) δ (ppm) 25.2, 26.1, 57.4, 64.8, 66.0, 72.9, 77.1, 109.4, 124.3, 125.0, 126.6, 129.2, 129.4, 130.6, 131.5, 171.1; UV λ_{max} 260 nm ($CHCl_3$); MS (EI) m/z 380 (M^+); HRMS (EI) $C_{23}H_{24}O_5$ found 380.16248, calcd 380.16237, Δm −0.11 mu.

Methyl 3-[(((*R*)-9-anthryl(methoxy)methyl)carbonyl)oxy]-2-(*R*)-methylpropanoate ((*R*)-10): HPLC t_R = 55.81 min (hexanes−ethyl acetate, 90:10, 2 mL/min, Spherisorb S5W 5 μm); [α] = −33.5 (c = 0.0055, EtOH); ^{1}H NMR (500.13 MHz, $CDCl_3$) δ (ppm) 0.69 (d, J = 7.1 Hz, 3H), 2.46 (m, 1H), 3.19 (s, 3H), 3.35 (s, 3H), 4.08 (m, 2H), 6.20 (s, 1H), 7.40 (m, 2H), 7.47 (m, 2H), 7.94 (d, J = 8.4 Hz, 2H), 8.41 (s, 1H), 8.46 (d, J = 9.0 Hz, 2H); ^{13}C NMR (75.47 MHz, $CDCl_3$) δ (ppm) 13.1, 38.7, 51.4, 57.5, 66.0, 77.1, 124.4, 125.0, 126.5, 127.0, 129.2, 130.5, 131.4, 170.9, 173.5; UV λ_{max} 260 nm ($CHCl_3$); MS (EI) m/z 366 (M^+); HRMS (EI) $C_{22}H_{22}O_5$ found 366.14624, calcd 366.14672, Δm 0.48 mu. Anal. Calcd for $C_{22}H_{22}O_5$: C, 72.1; H, 6.06. Found: C, 72.33; H, 5.89;

Methyl 3-[(((*S*)-9-anthryl(methoxy)methyl)carbonyl)oxy]-2-(*R*)-methylpropanoate ((*S*)-10): HPLC t_R = 57.45 min (hexanes−ethyl acetate, 90:10, 2 mL/min, Spherisorb S5W 5μm); [α] = +8.0 (c = 0.002, EtOH); ^{1}H NMR (500.13 MHz, $CDCl_3$) δ (ppm) 0.79 (d, J = 7.1 Hz, 3H), 2.36 (m, 1H), 3.09 (s, 3H), 3.34 (s, 3H), 4.08 (dd, J = 7.4, 10. Hz, 2H), 6.19 (s, 1H), 7.39 (m, 2H), 7.46 (m, 2H), 7.93 (d, J = 8.4 Hz, 2H), 8.39 (s, 1H), 8.46 (d, J = 9.2 Hz, 2H); ^{13}C NMR (75.47 MHz, $CDCl_3$) δ (ppm) 13.3, 38.6, 51.3, 57.5, 66.0, 77.1, 124.4, 125.0, 126.5, 127.0, 129.2, 130.5, 131.4, 170.9, 173.6; UV λ_{max} 260 nm ($CHCl_3$); MS (EI) m/z 366 (M^+); HRMS (EI) $C_{22}H_{22}O_5$ found 366.14668, calcd 366.14672 Δm 0.04 mu.

(+)-*trans*-Myrtanyl (*R*)-(−)-2-(9-anthryl)-2-methoxyacetate ((*R*)-11): HPLC t_R = 22.93 min (hexanes−ethyl acetate, 96:4, 2 mL/min, μ-porasil); [α] = −58.8 (c = 0.01, EtOH); ^{1}H NMR (500.13 MHz, $CDCl_3$) δ (ppm) 0.36 (s, 3H), 0.79 (s, 3H), 0.86 (m, 2H), 0.96 (td, J = 5.7, 1.0 Hz, 1H), 1.14 (m, 1H), 1.40 (m, 1H), 1.47 (m, 1H), 1.56 (m, 2H), 1.80 (m, 1H), 3.34 (s, 3H), 3.60 (dd, J = 8.4, 10.5 Hz, 1H), 3.89 (dd, J = 6.0, 10.5 Hz, 1H), 6.18 (s, 1H), 7.38 (m, 2H), 7.45 (m, 2H), 7.93 (d, J = 8.4 Hz, 2H), 8.38 (s, 1H), 8.47 (d, J = 9.0 Hz, 2H); ^{13}C NMR (75.47 MHz, $CDCl_3$) δ (ppm) 17.3, 19.6, 22.9, 23.7, 26.2, 33.9, 38.6, 40.4, 41.6, 57.4, 68.0, 77.2, 124.4, 125.0, 126.4, 127.4, 129.1, 130.5, 131.4, 171.4; UV λ_{max} 260 nm ($CHCl_3$); MS (EI) m/z 402 (M^+); HRMS (EI) $C_{27}H_{30}O_3$ found 402.21962, calcd 402.21950 Δm −0.12 mu. Anal. Calcd for $C_{27}H_{30}O_3$: C, 80.55; H, 7.52. Found: C, 80.73; H, 7.37.

(+)-*trans*-Myrtanyl (*S*)-(+)-2-(9-anthryl)-2-methoxyacetate ((*S*)-11): HPLC t_R = 22.75 min (hexanes−ethyl acetate, 96:4, 2 mL/min, μ-porasil); [α] = +89.7 (c = 0.007, EtOH); ^{1}H NMR (500.13 MHz, $CDCl_3$) δ (ppm) 0.46 (s, 3H), 0.79 (m, 1H), 0.83 (m, 1H), 0.85 (s, 3H), 1.07 (m, 2H), 1.39 (m, 1H), 1.48 (m, 1H), 1.57 (m, 2H), 1.85 (m, 1H), 3.35 (s, 3H), 3.73 (dd, J = 6.4, 10.6 Hz, 1H), 3.80 (dd, J = 7.3, 10.6 Hz, 1H), 6.18 (s, 1H), 7.38 (m, 2H), 7.45 (m, 2H), 7.93 (d, J = 8.4 Hz, 2H), 8.38 (s, 1H), 8.47 (d, J = 9.2 Hz, 2H); ^{13}C NMR (62.97 MHz, $CDCl_3$) δ (ppm) 17.4, 19.8, 22.9, 23.6, 26.2, 34.0, 38.7, 40.4, 41.9, 57.4, 68.6, 77.2, 124.5, 125.0, 126.4, 127.5, 129.1, 130.6, 131.5, 171.5; UV λ_{max} 260 nm ($CHCl_3$); MS (EI) m/z 402 (M^+); HRMS (EI) $C_{27}H_{30}O_3$ found 402.21934, calcd 402.21950, Δm 0.16 mu.

3-Bromo-2-(*R*)-(−)-methylpropyl (*R*)-(−)-2-(9-anthryl)-2-methoxyacetate ((*R*)-12): HPLC t_R = 24.81 min (hexanes−ethyl acetate, 94:6, 1 mL/min, Spherisorb S5W 5μm); [α] = +30.9 (c = 0.0065, EtOH); ^{1}H NMR (500.13 MHz, $CDCl_3$) δ (ppm) 0.43 (d, J = 6.8 Hz, 3H), 1.73 (m, 1H), 2.65 (dd, J = 5.5, 10.2 Hz, 1H), 2.74 (dd, J = 6.0, 10.5 Hz, 1H), 3.34 (s, 3H), 3.89 (m, 2H), 6.21 (s, 1H), 7.36 (m, 2H), 7.44 (m, 2H), 7.89 (d, J = 8.4 Hz, 2H), 8.36 (s, 1H), 8.46 (d, J = 9.2 Hz, 2H); ^{13}C NMR (62.97 MHz, $CDCl_3$) δ (ppm) 14.9, 34.2, 35.8, 57.4, 66.9, 77.1, 124.2, 125.0, 126.6, 127.2, 129.2, 130.5, 131.4, 171.1; UV λ_{max} 260 nm ($CHCl_3$); MS (EI) m/z 400 (M^+); HRMS (EI) $C_{21}H_{21}O_3Br$ found 400.06732, calcd 400.06741, Δm 0.09 mu. Anal. Calcd for $C_{21}H_{21}O_3Br$: C, 62.99; H, 5.29. Found: C, 63.25; H, 5.07.

3-Bromo-2-(*R*)-(−)-methylpropyl (*S*)-(+)-2-(9-anthryl)-2-methoxyacetate ((*S*)-12): HPLC t_R = 27.85 min (hexanes−ethyl acetate, 94:6, 1 mL/min, Spherisorb S5W 5μm); [α] = −40.0 (c = 0.003, EtOH); ^{1}H NMR (500.13 MHz, $CDCl_3$) δ (ppm) 0.60 (d, J = 6.8 Hz, 3H), 1.70 (m, 1H), 2.65 (d, J = 5.2 Hz, 2H), 3.38 (s, 3H), 3.82 (dd, J = 7.3, 11.2 Hz, 1H), 4.04 (dd, J = 5.2, 11.0 Hz, 1H), 6.24 (s, 1H), 7.41 (m, 2H), 7.49 (m, 2H), 7.95 (d, J = 8.5 Hz, 2H), 8.41 (s, 1H), 8.50 (d, J = 9.3 Hz, 2H); ^{13}C NMR (75.47 MHz, $CDCl_3$) δ (ppm) 15.1, 34.4, 35.9, 57.5, 67.0, 77.1, 124.3, 125.0, 126.6, 129.2, 129.3, 130.5, 131.4, 171.1; UV λ_{max} 260 nm ($CHCl_3$); MS (EI) m/z 400 (M^+); HRMS (EI) $C_{21}H_{21}O_3Br$ found 400.06753, calcd 400.06741, Δm −0.12 mu.

Boc-L-Alanyl (*R*)-(−)-2-(9-anthryl)-2-methoxyacetate ((R)-13): HPLC t_R = 31.89 min (hexanes−ethyl acetate, 85:15, 3 mL/min, μ-porasil); [α] = −114.9 (c = 0.0285, $CHCl_3$); ^{1}H NMR (500.13 MHz, $CDCl_3$) δ (ppm) 0.54 (d, J = 6.8 Hz, 3H), 1.27 (s, 9H), 3.36 (s, 3H), 3.56 (br, 1H), 3.78 (br, 1H), 3.89 (dd, J = 4.1, 10.6 Hz, 1H), 3.96 (br, 1H), 6.22 (s, 1H), 7.40 (m, 2H), 7.48 (m, 2H), 7.94 (d, J = 8.4 Hz, 2H), 8.40 (s, 1H), 8.49 (d, J = 9.2 Hz, 2H); ^{13}C NMR (75.47 MHz, $CDCl_3$) δ (ppm) 17.0, 28.3, 57.5, 67.4, 77.2, 124.3, 125.1, 126.7, 127.2, 129.2, 129.3, 130.5, 131.4, 154.8, 171.1; UV λ_{max} 258 nm ($CHCl_3$); MS (EI) m/z 423 (M^+); HRMS (EI) $C_{25}H_{29}O_5N$ found 423.20440, calcd 423.20457, Δm 0.17 mu. Anal. Calcd for $C_{25}H_{29}O_5N$: C, 70.9; H, 6.9; N, 3.31. Found: C, 71.23; H, 6.68; N, 3.52

Boc-L-Alanyl (*S*)-(+)-2-(9-anthryl)-2-methoxyacetate ((*S*)-13): HPLC t_R = 32.79 min (hexanes−ethyl acetate, 85:15, 3 mL/min, μ-porasil); [α] = +50.0 (c = 0.01, $CHCl_3$); ^{1}H NMR (500.13 MHz, $CDCl_3$) δ (ppm) 0.49 (br, 3H), 1.30 (s, 9H), 3.39 (s, 3H), 3.63 (br, 1H), 3.88 (dd, J = 4.4, 10.9 Hz, 1H), 3.96 (br, 2H), 6.24 (s, 1H), 7.41 (m, 2H), 7.48 (m, 2H), 7.95 (d, J = 8.4 Hz, 2H), 8.41 (s, 1H), 8.50 (d, J = 9.2 Hz, 2H); ^{13}C NMR (75.47 MHz, $CDCl_3$) δ (ppm) 16.8, 28.2, 57.5, 67.6, 77.2, 124.3, 125.0, 126.6, 127.1, 129.1, 129.2, 130.4, 131.4, 154.8, 171.0; UV λ_{max} 258 nm ($CHCl_3$); MS (EI) m/z 423 (M^+); HRMS (EI) $C_{25}H_{29}O_5N$ found 423.20406, calcd 423.20457, Δm 0.51 mu.

Boc-L-Valyl (*R*)-(−)-2-(9-anthryl)-2-methoxyacetate ((*R*)-14): HPLC t_R = 21.91 min (hexanes−ethyl acetate, 85:15, 3 mL/min, μ-porasil); [α] = −80.4 (c = 0.005, $CHCl_3$); ^{1}H NMR (500.13 MHz, $CDCl_3$) δ (ppm) 0.44 (d, J = 6.7 Hz, 3H), 0.49 (d, J = 6.8 Hz, 3H), 0.98 (m, 1H), 1.29 (s, 9H), 3.25 (m, 1H), 3.38 (s, 3H), 3.79 (d, J = 9.7 Hz, 1H), 4.00 (m, 2H), 6.21 (s, 1H), 7.41 (m, 2H), 7.49 (m, 2H), 7.96 (d, J = 8.4 Hz, 2H), 8.42 (s, 1H), 8.48 (d, J = 9.3 Hz, 2H); ^{13}C NMR (75.47 MHz, $CDCl_3$) δ (ppm) 17.9, 19.0, 28.3, 29.1, 54.5, 57.5, 64.9, 77.2, 79.1, 124.3, 125.0, 126.6, 127.2, 129.2, 130.5, 131.4, 155.4, 171.1; UV λ_{max} 258 nm ($CHCl_3$); MS (EI) m/z 451 (M^+); HRMS (EI) $C_{27}H_{33}O_5N$ found 451.23519, calcd 451.23587, Δm 0.68 mu. Anal. Calcd for $C_{27}H_{33}O_5N$: C, 71.82; H, 7.37; N, 3.1. Found: C, 71.98; H, 7.13; N, 2.88.

Boc-L-Valyl (*S*)-(+)-2-(9-anthryl)-2-methoxyacetate ((*S*)-14): HPLC t_R = 22.82 min (hexanes−ethyl acetate, 85:15, 3 mL/min, μ-porasil); [α] = +28.0 (c = 0.016, $CHCl_3$); ^{1}H NMR (500.13 MHz, $CDCl_3$) δ (ppm) 0.30 (d, J = 6.7 Hz, 3H), 0.39 (d, J = 6.7 Hz, 3H), 0.76 (m, 1H), 1.31 (s, 9H), 3.28 (m, 1H), 3.41 (s, 3H), 3.95 (d, J = 9.7 Hz, 1H), 3.98 (m, 2H), 6.22 (s, 1H), 7.40 (m, 2H), 7.48 (m, 2H), 7.94 (d, J = 8.4 Hz, 2H), 8.40 (s, 1H), 8.50 (d, J = 9.2 Hz, 2H); ^{13}C NMR (75.47 MHz, $CDCl_3$) δ (ppm) 18.1, 18.6, 28.2, 29.1, 54.2, 57.6, 65.2, 77.2, 79.1, 124.3, 125.0, 126.6, 127.1, 129.1, 130.4, 131.4, 155.3, 170.9; UV λ_{max} 258 nm ($CHCl_3$); MS (EI) m/z 451 (M^+); HRMS (EI) $C_{27}H_{33}O_5N$ found 451.23570, calcd 451.23587, Δm 0.17 mu.

Boc-L-Leucyl (*R*)-(−)-2-(9-anthryl)-2-methoxyacetate ((*R*)-15): HPLC t_R = 17.33 min (hexanes−ethyl acetate, 85:15, 3 mL/min, μ-porasil); [α] = −87.0 (c = 0.008, $CHCl_3$); ^{1}H NMR (500.13 MHz, $CDCl_3$) δ (ppm) 0.39 (m, 1H), 0.40 (d, J = 6.7 Hz, 3H), 0.48 (d, J = 6.7 Hz, 3H), 0.51 (m, 1H), 1.10 (m, 1H), 1.28 (s, 9H), 3.38 (s, 3H), 3.44 (m, 1H), 3.58 (d, J = 8.9 Hz, 1H), 3.81 (dd, J = 3.9, 11.2 Hz, 1H), 4.08 (dd, J = 4.7, 11.2 Hz, 1H), 6.22 (s, 1H), 7.41 (m, 2H), 7.49 (m, 2H), 7.96 (d, J = 8.4 Hz, 2H), 8.42 (s, 1H), 8.49 (d, J = 9.2 Hz, 2H); ^{13}C NMR (75.47 MHz, $CDCl_3$) δ (ppm) 21.6, 22.5, 24.1, 28.3, 39.9, 47.6, 57.5, 66.5, 77.2, 79.2, 124.3, 125.1, 126.7, 129.2, 130.4, 131.5, 155.0, 166.4, 171.0; UV λ_{max} 258 nm ($CHCl_3$); MS (EI) m/z 465 (M^+); HRMS (EI) $C_{28}H_{35}O_5N$ found 465.25122, calcd 465.25152, Δm 0.30 mu. Anal. Calcd for $C_{28}H_{35}O_5N$: C, 72.23; H, 7.58; N, 3.01. Found: C, 72.53; H, 7.23; N, 2.93.

Boc-L-Leucyl (*S*)-(+)-2-(9-anthryl)-2-methoxyacetate ((*S*)-15): HPLC t_R = 17.48 min (hexanes−ethyl acetate, 85:15, 3 mL/min, μ-porasil); [α] = +17.0 (c = 0.014, $CHCl_3$); ^{1}H NMR (500.13 MHz,

$CDCl_3$) δ (ppm) 0.32 (m, 1H), 0.34 (d, $J = 6.7$ Hz, 3H), 0.40 (m, 1H), 0.44 (d, $J = 6.7$ Hz, 3H), 0.98 (m, 1H), 1.30 (s, 9H), 3.40 (s, 3H), 3.52 (br, 1H), 3.76 (d, $J = 8.9$ Hz, 1H), 3.91 (dd, $J = 3.9$, 11.2 Hz, 1H), 3.97 (dd, $J = 3.8$, 11.2 Hz, 1H), 6.24 (s, 1H), 7.41 (m, 2H), 7.48 (m, 2H), 7.95 (d, $J = 8.7$ Hz, 2H), 8.41 (s, 1H), 8.52 (d, $J = 8.9$ Hz, 2H); ^{13}C NMR (75.47 MHz, $CDCl_3$) δ (ppm) 21.8, 22.2, 24.2, 28.3, 39.8, 47.4, 57.6, 66.7, 77.2, 79.2, 124.4, 125.0, 126.6, 129.2, 130.4, 131.4, 155.0, 166.4, 170.9; UV λ_{max} 258 nm ($CHCl_3$); MS (EI) *m*/*z* 465 (M^+); HRMS (EI) $C_{28}H_{35}O_5N$ found 465.25158, calcd 465.25152, Δm −0.06 mu.

Boc-L-Isoleucyl (*R*)-(−)-2-(9-anthryl)-2-methoxyacetate ((*R*)-16): HPLC t_R = 15.25 min (hexanes−ethyl acetate, 85:15, 3 mL/min, μ-porasil); [α] = −75.8 (c = 0.010, $CHCl_3$); ^{1}H NMR (500.13 MHz, $CDCl_3$) δ (ppm) 0.40 (d, $J = 6.3$ Hz, 3H), 0.46 (t, $J = 7.4$ Hz, 3H), 0.63 (m, 2H), 0.94 (m, 1H), 1.29 (s, 9H), 3.29 (m, 1H), 3.38 (s, 3H), 3.73 (d, $J = 9.3$ Hz, 1H), 3.98 (dd, $J = 4.5$, 11.5 Hz, 1H), 4.06 (dd, $J = 4.3$, 11.5 Hz, 1H), 6.22 (s, 1H), 7.41 (m, 2H), 7.49 (m, 2H), 7.95 (d, $J = 8.4$ Hz, 2H), 8.41 (s, 1H), 8.48 (d, $J = 9.2$ Hz, 2H); ^{13}C NMR (75.47 MHz, $CDCl_3$) δ (ppm) 11.0, 14.9, 24.7, 28.2, 35.6, 53.4, 57.5, 64.7, 77.1, 79.1, 124.2, 125.0, 126.6, 127.2, 129.1, 130.4, 131.4, 155.2, 171.0; UV λ_{max} 258 nm ($CHCl_3$); MS (EI) *m*/*z* 465 (M^+); HRMS (EI) $C_{28}H_{35}O_5N$ found 465.25144, calcd 465.25152, Δm 0.08 mu. Anal. Calcd for $C_{28}H_{35}O_5N$: C, 72.23; H, 7.58; N, 3.01. Found: C, 72.23; H, 7.58; N, 2.57.

Boc-L-Isoleucyl (*S*)-(+)-2-(9-anthryl)-2-methoxyacetate ((*S*)-16): HPLC t_R = 15.43 min (hexanes−ethyl acetate, 85:15, 3 mL/min, μ-porasil); [α] = +15.2 (c = 0.015, $CHCl_3$); ^{1}H NMR (500.13 MHz, $CDCl_3$) δ (ppm) 0.15 (d, $J = 6.7$ Hz, 3H), 0.35 (m, 1H), 0.41 (t, $J = 7.3$ Hz, 3H), 0.58 (m, 1H), 0.91 (m, 1H), 1.31 (s, 9H), 3.31 (m, 1H), 3.42 (s, 3H), 3.92 (d, $J = 9.6$ Hz, 1H), 3.96 (dd, $J = 4.5$, 11.5 Hz, 1H), 4.01 (dd, $J = 4.2$, 11.3 Hz, 1H), 6.23 (s, 1H), 7.41 (m, 2H), 7.48 (m, 2H), 7.95 (d, $J = 8.3$ Hz, 2H), 8.41 (s, 1H), 8.51 (d, $J = 9.2$ Hz, 2H); ^{13}C NMR (75.47 MHz, $CDCl_3$) δ (ppm) 10.8, 14.4, 24.7, 28.2, 35.4, 53.1, 57.5, 65.0, 77.1, 79.0, 124.2, 124.9, 126.5, 127.0, 129.0, 130.3, 131.3, 155.2, 170.8; UV λ_{max} 258 nm ($CHCl_3$); MS (EI) *m*/*z* 465 (M^+); HRMS (EI) $C_{28}H_{35}O_5N$ found 465.25168, calcd 465.25152, Δm −0.16 mu.

Boc-L-phenylalanyl (*R*)-(−)-2-(9-anthryl)-2-methoxyacetate ((*R*)-17): HPLC t_R = 21.20 min (hexanes−ethyl acetate, 85:15, 2 mL/min, μ-porasil); [α] = −73.8 (c = 0.025, $CHCl_3$); ^{1}H NMR (500.13 MHz, $CDCl_3$) δ (ppm) 1.34 (s, 9H), 1.71 (m, 1H), 2.06 (m, 1H), 3.48 (s, 3H), 3.71 (m, 2H), 3.82 (m, 1H), 4.17 (m, 1H), 6.32 (s, 1H), 6.46 (d, $J = 7.1$ Hz, 2H), 7.02 (m, 2H), 7.05 (m, 1H), 7.50 (m, 2H), 7.60 (m, 2H), 8.04 (d, $J = 8.4$ Hz, 2H), 8.50 (s, 1H), 8.59 (d, $J = 8.9$ Hz, 2H); ^{13}C NMR (62.97 MHz, $CDCl_3$) δ (ppm) 28.2, 36.6, 50.5, 57.6, 64.5, 77.1, 79.3, 124.3, 125.2, 126.4, 126.9, 127.5, 128.3, 128.8, 129.0, 129.4, 130.5, 131.5, 136.7, 154.9, 171.1; UV λ_{max} 262 nm ($CHCl_3$); MS (EI) *m*/*z* 499 (M^+); HRMS (EI) $C_{31}H_{33}O_5N$ found 499.23572, calcd 499.23587, Δm 0.15 mu. Anal. Calcd for $C_{31}H_{33}O_5N$: C, 74.51; H, 6.66; N, 2.8. Found: C, 74.62; H, 6.50; N, 2.85.

Boc-L-phenylalanyl (*S*)-(+)-2-(9-anthryl)-2-methoxyacetate ((*S*)-17): HPLC t_R = 22.00 min (hexanes−ethyl acetate, 85:15, 2 mL/min, μ-porasil); [α] = +54.2 (c = 0.0145, $CHCl_3$); ^{1}H NMR (500.13 MHz, $CDCl_3$) δ (ppm) 1.37 (s, 9H), 1.65 (m, 1H), 2.11 (m, 1H), 3.49 (s, 3H), 3.75 (br, 1H), 3.81 (dd, $J = 3.4$, 11.3 Hz, 1H), 3.95 (m, 1H), 4.18 (m, 1H), 6.25 (d, $J = 7.0$ Hz, 2H), 6.37 (s, 1H), 6.89 (t, $J = 7.6$ Hz, 2H), 7.00 (t, $J = 7.4$ Hz, 1H), 7.51 (m, 2H), 7.60 (m, 2H), 8.05 (d, $J = 8.4$ Hz, 2H), 8.52 (s, 1H), 8.64 (d, $J = 8.7$ Hz, 2H); ^{13}C NMR (62.97 MHz, $CDCl_3$) δ (ppm) 28.2, 36.9, 50.3, 57.6, 64.9, 77.3, 79.5, 124.4, 125.2, 126.3, 126.8, 127.3, 128.2, 128.8, 129.4, 129.5, 130.5, 131.6, 136.7, 154.9, 170.7; UV λ_{max} 262 nm ($CHCl_3$); MS (EI) *m*/*z* 499 (M^+); HRMS (EI) $C_{31}H_{33}O_5N$ found 499.23574, calcd 499.23587, Δm 0.13 mu.

(*R*)-γ-Hydroxymethyl-γ-butyrolactone (*R*)-(−)-2-(9-anthryl)-2-methoxyacetate ((*R*)-18): HPLC t_R = 22.50 min (hexanes−ethyl acetate, 40:60, 1 mL/min, Spherisorb S5W 5μm); [α] = −93.0 (c = 0.0145, $CHCl_3$); ^{1}H NMR (500.13 MHz, $CDCl_3$) δ (ppm) 0.89 (m, 1H), 1.15 (m, 1H), 1.62 (m, 1H), 1.79 (m, 1H), 3.38 (s, 3H), 4.00 (dd, $J = 3.1$, 12.2 Hz, 1H), 4.19 (dd, $J = 2.9$, 12.2 Hz, 1H), 4.39 (m, 1H), 6.25 (s, 1H), 7.42 (m, 2H), 7.50 (m, 2H), 7.96 (d, $J = 8.3$ Hz, 2H), 8.43 (s, 1H), 8.45 (d, $J = 9.0$ Hz, 2H); ^{13}C NMR (75.47 MHz, $CDCl_3$) δ (ppm) 22.6, 27.0, 57.6, 65.5, 76.3, 76.8, 124.0, 125.2, 126.7, 126.9, 129.2, 129.4, 130.4, 131.3, 171.0, 176.2; UV λ_{max} 266 nm ($CHCl_3$); MS (EI) *m*/*z* 364 (M^+); HRMS (EI) $C_{22}H_{20}O_5$ found 364.13114, calcd 364.13107, Δm −0.07 mu. Anal. Calcd for $C_{22}H_{20}O_5$: C, 72.51; H, 5.53. Found: C, 72.78; H, 5.27.

(*R*)-γ-Hydroxymethyl-γ-butyrolactone (*S*)-(+)-2-(9-anthryl)-2-methoxyacetate ((*S*)-18): HPLC t_R = 23.65 min (hexanes−ethyl acetate, 40:60, 1 mL/min, Spherisorb S5W 5μm); [α] = +50.1 (c = 0.034, $CHCl_3$); ^{1}H NMR (500.13 MHz, $CDCl_3$) δ (ppm) 1.48 (m, 1H), 1.81 (m, 1H), 1.85 (m, 1H), 2.05 (m, 1H), 3.34 (s, 3H), 4.03 (dd, $J = 5.2$, 12.2 Hz, 1H), 4.13 (dd, $J = 3.5$, 12.2 Hz, 1H), 4.26 (m, 1H), 6.23 (s, 1H), 7.38 (m, 2H), 7.45 (m, 2H), 7.93 (d, $J = 8.3$ Hz, 2H), 8.40 (s, 1H), 8.43 (d, $J = 9.0$ Hz, 2H); ^{13}C NMR (75.47 MHz, $CDCl_3$) δ (ppm) 23.3, 27.3, 57.5, 65.6, 76.5, 76.9, 124.0, 125.0, 126.7, 129.2, 129.5, 130.4, 131.4, 170.9, 175.8; UV λ_{max} 266 nm ($CHCl_3$); MS (EI) *m*/*z* 364 (M^+); HRMS (EI) $C_{22}H_{20}O_5$ found 364.13117, calcd 364.13107, Δm −0.10 mu.

(*S*)-5-(Hydroxymethyl)-2-pyrrolidinone (*R*)-(−)-2-(9-anthryl)-2-methoxyacetate ((*R*)-19): [α] = −39.7 (c = 0.0175, $CHCl_3$); ^{1}H NMR (500.13 MHz, $CDCl_3$) δ (ppm) 1.42 (m, 1H), 1.90 (m, 1H), 2.04 (m, 2H), 3.42 (s, 3H), 3.47 (m, 1H), 3.80 (dd, $J = 7.9$, 11.2 Hz, 1H), 4.16 (dd, $J = 3.9$, 11.2 Hz, 1H), 5.65 (br, 1H), 6.35 (s, 1H), 7.49 (m, 2H), 7.55 (m, 2H), 8.03 (d, $J = 7.9$ Hz, 2H), 8.50 (s, 1H), 8.53 (d, $J = 9.0$ Hz, 2H); ^{13}C NMR (75.47 MHz, $CDCl_3$) δ (ppm) 22.5, 29.0, 52.3, 57.4, 67.4, 76.8, 124.0, 125.1, 126.8, 129.3, 129.5, 130.4, 131.4, 171.1, 177.4; UV λ_{max} 264 nm ($CHCl_3$); MS (EI) *m*/*z* 363 (M^+); HRMS (EI) $C_{22}H_{21}O_4N$ found 363.14696, calcd 363.14705, Δm 0.09 mu. Anal. Calcd for $C_{22}H_{21}O_4N$: C, 72.71; H, 5.82; N, 3.85. Found: C, 72.83; H, 5.69; N, 3.56.

(*S*)-5-(Hydroxymethyl)-2-pyrrolidinone (*S*)-(+)-2-(9-anthryl)-2-methoxyacetate ((*S*)-19): [α] = +135.3 (c = 0.027, $CHCl_3$); ^{1}H NMR (500.13 MHz, $CDCl_3$) δ (ppm) 1.20 (m, 1H), 1.76 (m, 2H), 1.94 (m, 1H), 3.42 (s, 3H), 3.58 (m, 1H), 3.83 (dd, $J = 6.0$, 11.4 Hz, 1H), 4.10 (dd, $J = 4.0$, 11.3 Hz, 1H), 6.01 (br, 1H), 6.32 (s, 1H), 7.47 (m, 2H), 7.55 (m, 2H), 8.02 (d, $J = 7.8$ Hz, 2H), 8.49 (s, 1H), 8.52 (d, $J = 8.9$ Hz, 2H); ^{13}C NMR (75.47 MHz, $CDCl_3$) δ (ppm) 22.5, 29.0, 52.2, 57.4, 67.1, 76.8, 124.0, 125.1, 126.7, 129.2, 129.4, 130.4, 131.3, 171.2, 177.7; UV λ_{max} 264 nm ($CHCl_3$); MS (EI) *m*/*z* 363 (M^+); HRMS (EI) $C_{22}H_{21}O_4N$ found 363.14708, calcd 363.14705, Δm −0.03 mu.

2,3-*O*,*O*′-Isopropilidene-D-ribono-1,4-lactone (*R*)-(−)-2-(9-anthryl)-2-methoxyacetate ((*R*)-20): HPLC t_R = 19.45 min (hexanes−ethyl acetate, 60:40, 2 mL/min, Spherisorb S5W 5μm); [α] = −67.3 (c = 0.0295, $CHCl_3$); ^{1}H NMR (500.13 MHz, $CDCl_3$) δ (ppm) 1.17 (s, 3H), 1.28 (s, 3H), 3.30 (d, $J = 5.8$ Hz, 1H), 3.41 (s, 3H), 4.09 (dd, $J = 2.2$, 12.2 Hz, 1H), 4.29 (d, $J = 5.8$ Hz, 1H), 4.44 (dd, $J = 2.5$, 12.0 Hz, 1H), 4.46 (t, $J = 2.4$ Hz, 1H), 6.30 (s, 1H), 7.50 (m, 2H), 7.56 (m, 2H), 8.07 (d, $J = 7.7$ Hz, 2H), 8.42 (d, $J = 8.9$ Hz, 2H), 8.55 (s, 1H); ^{13}C NMR (62.97 MHz, $CDCl_3$) δ (ppm) 25.1, 26.4, 57.4, 63.9, 74.0, 76.6, 76.9, 78.9, 113.3, 123.3, 125.1, 127.0, 129.6, 129.9, 130.3, 131.3, 170.4, 172.1; UV λ_{max} 260 nm ($CHCl_3$); MS (EI) *m*/*z* 436 (M^+); HRMS (EI) $C_{25}H_{24}O_7$ found 436.15209, calcd 436.15220, Δm 0.11 mu. Anal. Calcd for $C_{25}H_{24}O_7$: C, 68.8; H, 5.54. Found: C, 69.12; H, 5.28.

2,3-*O*,*O*′-Isopropilidene-D-ribono-1,4-lactone(*S*)-(+)-2-(9-anthryl)-2-methoxyacetate ((*S*)-20): HPLC t_R = 16.49 min (hexanes−ethyl acetate, 60:40, 2 mL/min, Spherisorb S5W 5μm); [α] = +68.9 (c = 0.024, $CHCl_3$); ^{1}H NMR (500.13 MHz, $CDCl_3$) δ (ppm) 0.85 (s, 3H), 1.20 (s, 3H), 2.15 (d, $J = 5.8$ Hz, 1H), 3.24 (d, $J = 5.8$ Hz, 1H), 3.48 (s, 3H), 4.17 (dd, $J = 2.1$, 12.5 Hz, 1H), 4.27 (dd, $J = 1.8$, 12.5 Hz, 1H), 4.39 (t, $J = 1.9$ Hz, 1H), 6.27 (s, 1H), 7.53 (m, 2H), 7.60 (m, 2H), 8.06 (d, $J = 7.9$ Hz, 2H), 8.42 (d, $J = 8.5$ Hz, 2H), 8.56 (s, 1H); ^{13}C NMR (62.97 MHz, $CDCl_3$) δ (ppm) 24.4, 26.2, 57.7, 64.2, 73.7, 76.2, 76.7, 79.0, 113.0, 123.3, 125.5, 126.5, 127.5, 129.4, 129.5, 130.3, 131.2, 170.7, 172.5; UV λ_{max} 260 nm ($CHCl_3$); MS (EI) *m*/*z* 436 (M^+); HRMS (EI) $C_{25}H_{24}O_7$ found 436.15204, calcd 436.15220, Δm 0.16 mu.

(2*R*,3*R*)-*trans*-3-Phenyloxirane-2-methyl (*R*)-(−)-2-(9-anthryl)-2-methoxyacetate ((*R*)-21): HPLC t_R = 11.45 min (hexanes−ethyl acetate, 75:25, 2 mL/min, μ-porasil); [α] = −56.7 (c = 0.030, EtOH); ^{1}H NMR (500.13 MHz, $CDCl_3$) δ (ppm) 2.77 (m, 1H), 3.27 (d, $J = 1.9$ Hz, 1H), 3.34 (s, 3H), 4.05 (dd, $J = 5.2$, 12.2 Hz, 1H), 4.26 (dd, $J = 3.8$, 12.2 Hz, 1H), 6.25 (s, 1H), 6.87 (m, 2H), 7.14 (m, 3H), 7.38 (m, 4H), 7.91 (d, $J = 8.3$ Hz, 2H), 8.38 (s, 3H), 8.45 (d, $J = 8.8$ Hz,

2H); ^{13}C NMR (62.97 MHz, $CDCl_3$) δ (ppm) 56.2, 57.5, 58.5, 64.6, 77.0, 124.3, 125.1, 125.6, 126.7, 126.9, 128.3, 128.4, 129.2, 129.5, 130.6, 131.5, 136.0, 171.2; UV λ_{max} 260 nm ($CHCl_3$); MS (EI) *m*/*z* 398 (M^+); HRMS (EI) $C_{26}H_{22}O_4$ found 398.15222, calcd 398.15185, Δm 0.37 mu. Anal. Calcd for $C_{26}H_{22}O_4$: C, 78.36; H, 5.57. Found: C, 78.61; H, 5.24.

(2*R*,3*R*)-*trans*-3-Phenyloxirane-2-methyl (*S*)-(+)-2-(9-anthryl)-2-methoxyacetate ((*S*)-21): HPLC t_R = 11.62 min (hexanes−ethyl acetate, 75:25, 2 mL/min, μ-porasil); [α] = +85.7 (*c* = 0.015, EtOH); ^{1}H NMR (500.13 MHz, $CDCl_3$) δ (ppm) 2.98 (m, 1H), 3.18 (d, *J* = 2.2 Hz, 1H), 3.36 (s, 3H), 4.04 (dd, *J* = 4.2, 12.5 Hz, 2H), 4.37 (dd, *J* = 3.2, 12.5 Hz, 1H), 6.27 (s, 1H), 6.80 (m, 2H), 7.16 (m, 3H), 7.40 (m, 2H), 7.47 (m, 2H), 7.95 (d, *J* = 8.4 Hz, 2H), 8.42 (s, 1H), 8.50 (d, *J* = 8.9 Hz, 2H); ^{13}C NMR (75.47 MHz, $CDCl_3$) δ (ppm) 55.7, 57.5, 58.8, 63.5, 77.0, 124.3, 125.0, 125.5, 126.7, 126.8, 128.3, 128.4, 129.2, 129.5, 130.5, 131.5, 135.9, 171.0; UV λ_{max} 260 nm ($CHCl_3$); MS (EI) *m*/*z* 398 (M^+); HRMS (EI) $C_{26}H_{22}O_4$ found 398.15185, calcd 398.15185, Δm 0.00 mu.

(−)-Isolongifolyl (*R*)-(−)-2-(9-anthryl)-2-methoxyacetate ((*R*)-22): HPLC t_R = 20.77 min (hexanes−ethyl acetate, 93:7, 2 mL/min, Spherisorb S5W 5μm); [α] = −75.4 (*c* = 0.016, EtOH); ^{1}H NMR (500.13 MHz, $CDCl_3$) δ (ppm) 0.13 (s, 3H), 0.55 (m, 1H), 0.61 (s, 3H), 0.72 (m, 1H), 0.82 (s, 3H), 1.1 (m, 6H), 1.32 (m, 2H), 1.63 (br, 1H), 1.72 (br, 1H), 1.81 (m, 1H), 3.41 (s, 3H), 4.03 (m, 2H), 6.26 (s, 1H), 7.42 (m, 2H), 7.50 (m, 2H), 7.96 (d, *J* = 8.3 Hz, 2H), 8.41 (s, 1H), 8.58 (d, *J* = 8.9 Hz, 2H); ^{13}C NMR (62.97 MHz, $CDCl_3$) δ (ppm) 21.3, 22.4, 25.7, 29.2, 32.6, 33.0, 39.6, 40.0, 41.1, 43.3, 45.5, 57.4, 61.6, 64.6, 77.1, 124.7, 125.0, 126.4, 127.3, 127.5, 129.1, 130.7, 131.6, 171.1; UV λ_{max} 260 nm ($CHCl_3$); MS (EI) *m*/*z* 470 (M^+); HRMS (EI) $C_{32}H_{38}O_3$ found 470.28142, calcd 470.28210, Δm 0.68 mu. Anal. Calcd for $C_{32}H_{38}O_3$: C, 81.65; H, 8.14. Found: C, 81.91; H, 8.01.

(−)-Isolongifolyl (*S*)-(+)-2-(9-anthryl)-2-methoxyacetate ((*S*)-22): HPLC t_R = 21.77 min (hexanes−ethyl acetate, 93:7, 2 mL/min, Spherisorb S5W 5μm); [α] = +14.2 (*c* = 0.023, EtOH); ^{1}H NMR (500.13 MHz, $CDCl_3$) δ (ppm) 0.31 (s, 3H), 0.38 (m, 1H), 0.38 (s, 3H), 0.55 (m, 1H), 0.65 (s, 3H), 0.70 (m, 2H), 0.87 (m, 5H), 1.01 (m, 1H), 1.16 (m, 2H), 1.51 (m, 2H), 3.29 (s, 3H), 3.73 (dd, *J* = 7.6, 10.9 Hz, 1H), 4.12 (dd, *J* = 8.1, 10.8 Hz, 1H), 6.12 (s, 1H), 7.29 (m, 2H), 7.37 (m, 2H), 7.83 (d, *J* = 8.5 Hz, 2H), 8.28 (s, 1H), 8.43 (d, *J* = 8.8 Hz, 2H); ^{13}C NMR (75.47 MHz, $CDCl_3$) δ (ppm) 21.2, 22.2, 25.6, 29.1, 32.5, 32.9, 39.4, 39.8, 40.9, 43.1, 45.3, 45.4, 57.3, 61.4, 64.5, 77.3, 124.5, 124.8, 126.3, 127.3, 128.9, 130.4, 131.4, 170.9; UV λ_{max} 260 nm ($CHCl_3$); MS (EI) *m*/*z* 470 (M^+); HRMS (EI) $C_{32}H_{38}O_3$ found 470.28230, calcd 470.28210, Δm −0.20 mu.

1,2:3,4-Di-*O*,*O*′,*O*″,*O*‴-isopropylidene-α-D-galactopyranosyl (*R*)-(−)-2-(9-anthryl)-2-methoxyacetate ((*R*)-23): HPLC t_R = 39.69 min (hexanes−ethyl acetate, 85:15, 2 mL/min, Spherisorb S5W 5μm); [α] = −133.0 (*c* = 0.008, $CHCl_3$); ^{1}H NMR (500.13 MHz, $CDCl_3$) δ (ppm) 1.06 (s, 3H), 1.13 (s, 3H), 1.24 (s, 3H), 1.35 (s, 3H), 3.43 (s, 3H), 3.65 (dq, *J* = 1.9, 4.1 Hz, 1H), 3.77 (dd, *J* = 1.9, 7.9 Hz, 1H), 4.06 (dd, *J* = 4.1, 11.6 Hz, 1H), 4.18 (dd, *J* = 2.5, 4.9 Hz, 1H), 4.34 (dd, *J* = 7.7, 11.6 Hz, 1H), 4.39 (dd, *J* = 2.5, 7.9 Hz, 1H), 5.42 (d, *J* = 4.9 Hz, 1H), 6.32 (s, 1H), 7.46 (m, 2H), 7.54 (m, 2H), 8.00 (d, *J* = 7.1 Hz, 2H), 8.46 (s, 1H), 8.69 (d, *J* = 8.9 Hz, 2H); ^{13}C NMR (62.97 MHz, $CDCl_3$) δ (ppm) 24.1, 24.9, 25.6, 25.8, 57.6, 64.4, 66.0, 70.4, 70.5, 70.8, 77.4, 96.0, 108.6, 109.5, 124.8, 125.0, 126.5, 129.0, 129.2, 130.6, 131.5, 171.0; UV λ_{max} 264 nm ($CHCl_3$); MS (EI) *m*/*z* 508 (M^+); HRMS (EI) $C_{29}H_{32}O_8$ found 508.21007, calcd 508.20971 Δm −0.36 mu. Anal. Calcd for $C_{29}H_{32}O_8$: C, 68.49; H, 6.34. Found: C, 68.73; H, 6.27.

1,2:3,4-Di-*O*,*O*′,*O*″,*O*‴-isopropylidene-α-D-galactopyranosyl (*S*)-(+)-2-(9-anthryl)-2-methoxyacetate ((*S*)-23): HPLC t_R = 34.41 min (hexanes−ethyl acetate, 85:15, 2 mL/min, Spherisorb S5W 5μm); [α] = +77.2 (*c* = 0.012, $CHCl_3$); ^{1}H NMR (500.13 MHz, $CDCl_3$) δ (ppm) 0.99 (s, 3H), 1.19 (s, 3H), 1.22 (s, 3H), 1.27 (s, 3H), 3.09 (d, *J* = 7.9 Hz, 1H), 3.42 (s, 3H), 3.63 (dt, *J* = 1.6, 6.8 Hz, 1H), 3.97 (dd, *J* = 7.0, 10.9 Hz, 1H), 4.07 (dd, *J* = 2.3, 4.9 Hz, 1H), 4.11 (dd, *J* = 2.3, 7.9 Hz, 1H), 4.24 (dd, *J* = 6.7, 10.9 Hz, 1H), 5.28 (d, *J* = 4.9 Hz, 1H), 6.24 (s, 1H), 7.42 (m, 2H), 7.48 (m, 2H), 7.96 (d, *J* = 7.7 Hz, 2H), 8.42 (s, 1H), 8.50 (d, *J* = 8.9 Hz, 2H); ^{13}C NMR (62.97 MHz, $CDCl_3$) δ (ppm) 23.7, 24.8, 25.6, 25.8, 57.6, 63.0, 64.5, 69.8, 70.2, 70.4, 77.1, 96.0, 108.5, 109.0, 124.4, 125.1, 126.7, 129.1, 129.2, 130.6, 131.5, 171.3; UV λ_{max} 264 nm ($CHCl_3$); MS (EI) *m*/*z* 508 (M^+); HRMS (EI) $C_{29}H_{32}O_8$ found 508.20996, calcd 508.20971, Δm −0.25 mu.

(*S*)-(−)-2-Methylbutyl (*R*)-(−)-2-methoxy-2-phenylacetate ((*R*)-24): HPLC t_R = 21.45 min (hexanes−ethyl acetate, 96:4, 2 mL/min, Spherisorb S5W 5μm); [α] = −68.2 (*c* = 0.009, EtOH); ^{1}H NMR (500.13 MHz, $CDCl_3$) δ (ppm) 0.82 (m, 6H), 1.09 (m, 1H), 1.30 (m, 1H), 1.66 (m, 1H), 3.42 (s, 3H), 3.96 (m, 2H), 4.77 (s, 1H), 7.37 (m, 3H), 7.45 (m, 2H); ^{1}H NMR (500.13 MHz, CS_2 + CD_2Cl_2 (4:1)) δ (ppm) 0.78 (d, *J* = 6.8 Hz, 3H), 0.83 (t, *J* = 7.5 Hz, 3H), 1.08 (m, 1H), 1.28 (m, 1H), 1.59 (m, 1H), 3.32 (s, 3H), 3.80 (dd, *J* = 6.6, 10.7 Hz, 1H), 3.90 (dd, *J* = 6.0, 10.7 Hz, 1H), 4.62 (s, 1H), 7.20−7.32 (m, 5H); ^{13}C NMR (62.97 MHz, $CDCl_3$) δ (ppm) 10.9, 16.0, 25.8, 34.0, 57.3, 69.6, 82.7, 127.2, 128.6, 128.7, 136.5, 170.9; UV λ_{max} 242 nm ($CHCl_3$); MS (EI) *m*/*z* 236 (M^+); HRMS (EI) $C_{14}H_{20}O_3$ found 236.14125, calcd 236.14125, Δm 0.00 mu. Anal. Calcd for $C_{14}H_{20}O_3$: C, 71.16; H, 8.53. Found: C, 71.50; H, 8.25.

(*S*)-(−)-2-Methylbutyl (*S*)-(+)-2-methoxy-2-phenylacetate ((*S*)-24): HPLC t_R = 21.57 min (hexanes−ethyl acetate, 96:4, 2 mL/min, Spherisorb S5W 5μm); [α] = +72.0 (*c* = 0.028, EtOH); ^{1}H NMR (500.13 MHz, $CDCl_3$) δ (ppm) 0.81 (m, 6H), 1.07 (m, 1H), 1.28 (m, 1H), 1.64 (m, 1H), 3.42 (s, 3H), 3.95 (m, 2H), 4.76 (s, 1H), 7.35 (m, 3H), 7.44 (m, 2H); ^{1}H NMR (500.13 MHz, CS_2 + CD_2Cl_2 (4:1)) δ (ppm) 0.79 (d, *J* = 6.8 Hz, 3H), 0.81 (t, *J* = 7.4 Hz, 3H), 1.06 (m, 1H), 1.27 (m, 1H), 1.58 (m, 1H), 3.32 (s, 3H), 3.81 (ddd, *J* = 1.3, 6.6, 10.7 Hz, 1H), 3.87 (ddd, *J* = 1.0, 5.9, 10.7 Hz, 1H), 4.62 (s, 1H), 7.20−7.32 (m, 5H); ^{13}C NMR (62.97 MHz, $CDCl_3$) δ (ppm) 10.9, 16.0, 25.7, 34.0, 57.2, 69.5, 82.6, 127.1, 128.5, 128.6, 136.5, 170.8; UV λ_{max} 242 nm ($CHCl_3$); MS (EI) *m*/*z* 236 (M^+); HRMS (EI) $C_{14}H_{20}O_3$ found 236.14120, calcd 236.14125, Δm −0.05 mu.

(*S*)-(−)-2-Methylbutyl (*R*)-(−)-2-methoxy-2-(trifluoromethyl)-2-phenylacetate ((*R*)-25): HPLC t_R = 22.79 min (hexanes−ethyl acetate, 96:4, 2 mL/min, Spherisorb S5W 5μm); [α] = +54.0 (*c* = 0.03, $CHCl_3$); ^{1}H NMR (500.13 MHz, CS_2 + CD_2Cl_2 (4:1)) δ (ppm) 0.89 (t, *J* = 7.4 Hz, 3H), 0.91 (d, *J* = 6.7 Hz, 3H), 1.17 (m, 1H), 1.37 (m, 1H), 1.72 (m, 1H), 3.47 (s, 3H), 4.07 (d, *J* = 6.1 Hz, 2H), 7.30−7.42 (m, 5H); ^{13}C NMR (75.47 MHz, $CDCl_3$) δ (ppm) 11.0, 16.3, 25.8, 34.0, 55.4, 70.9, 84.6 (*J* = 27.9 Hz), 117.6, 121.4, 125.3, 127.3, 128.4, 129.5, 132.4, 166.7; UV λ_{max} 232 nm ($CHCl_3$); MS (EI) *m*/*z* 304 (M^+); HRMS (EI) $C_{15}H_{19}O_3F_3$ found 304.12863, calcd 304.12862, Δm −0.01 mu. Anal. Calcd for $C_{15}H_{19}O_3F_3$: C, 59.2; H, 6.29. Found: C, 59.47; H, 6.56.

(*S*)-(−)-2-methylbutyl (*S*)-(+)-2-methoxy-2-(trifluoromethyl)-2-phenylacetate ((*S*)-25): HPLC t_R = 21.57 min (hexanes−ethyl acetate, 96:4, 2 mL/min, Spherisorb S5W 5μm); [α] = −43.0 (*c* = 0.035, $CHCl_3$); ^{1}H NMR (500.13 MHz, CS_2 + CD_2Cl_2 (4:1)) δ (ppm) 0.89 (t, *J* = 7.5 Hz, 3H), 0.90 (d, *J* = 6.8 Hz, 3H), 1.18 (m, 1H), 1.39 (m, 1H), 1.71 (m, 1H), 3.47 (s, 3H), 4.00 (dd, *J* = 6.6, 10.7 Hz, 1H), 4.15 (dd, *J* = 5.7, 10.7 Hz, 1H), 7.30−7.42 (m, 5H); ^{13}C NMR (75.47 MHz, $CDCl_3$) δ (ppm) 11.0, 16.2, 25.8, 33.9, 55.4, 70.9, 84.6 (*J* = 27.9 Hz), 117.6, 121.4, 125.3, 127.3, 128.3, 129.5, 132.4, 166.6; UV λ_{max} 232 nm ($CHCl_3$); MS (EI) *m*/*z* 304 (M^+); HRMS (EI) $C_{15}H_{19}O_3F_3$ found 304.12868, calcd 304.12862, Δm −0.06 mu.

D-α,β-Isopropylidenegliceryl (*R*)-(−)-2-methoxy-2-phenylacetate ((*R*)-26): HPLC t_R = 18.15 min (hexanes−ethyl acetate, 75:25, 2 mL/min, Spherisorb S5W 5μm); [α] = −46.0 (*c* = 0.0075, EtOH); ^{1}H NMR (250.13 MHz, $CDCl_3$) δ (ppm) 1.28 (s, 3H), 1.32 (s, 3H), 3.37 (s, 3H), 3.53 (dd, *J* = 5.6, 8.3 Hz, 1H), 3.88 (dd, *J* = 5.8, 8.4 Hz, 1H), 4.16 (m, 3H), 4.77 (s, 1H), 7.29−7.43 (m, 5H); ^{13}C NMR (62.97 MHz, $CDCl_3$) δ (ppm) 25.3, 26.5, 57.3, 64.7, 66.1, 73.3, 82.5, 110.0, 127.3, 128.7, 128.8, 136.2, 170.5; UV λ_{max} 260 nm ($CHCl_3$); MS (EI) *m*/*z* 280 (M^+). HRMS (EI) $C_{15}H_{20}O_5$ found 280.13101, calcd 280.13101, Δm 0.00 mu. Anal. Calcd for $C_{15}H_{20}O_5$: C, 64.27; H, 7.19. Found: C, 64.53; H, 7.02.

D-α,β-Isopropylidenegliceryl (*S*)-(+)-2-methoxy-2-phenylacetate ((*S*)-26): HPLC t_R = 18.47 min (hexanes−ethyl acetate, 75:25, 2 mL/min, Spherisorb S5W 5μm); [α] = +67.0 (*c* = 0.06, EtOH); ^{1}H NMR (250.13 MHz, $CDCl_3$) δ (ppm) 1.31 (s, 3H), 1.34 (s, 3H), 3.39 (s, 3H), 3.60 (m, 1H), 3.93 (m, 1H), 4.1 (m, 1H), 4.21 (m, 2H), 4.79 (s, 1H), 7.34 (m, 3H), 7.43 (m, 2H); ^{13}C NMR (62.97 MHz, $CDCl_3$) δ (ppm) 25.2, 26.4, 57.2, 65.0, 66.1, 73.1, 82.3, 109.7, 127.1, 128.6, 128.8, 136.0,

170.5; UV λ_{max} 260 nm ($CHCl_3$); MS (EI) *m*/*z* 280 (M^+); HRMS (EI) $C_{15}H_{20}O_5$ found 280.13103, calcd 280.13101, Δm −0.02 mu.

D-α,β-Isopropylidenegliceryl (*R*)-(−)-2-methoxy-2-(trifluoromethyl)-2-phenylacetate ((*R*)-27): HPLC t_R = 11.32 min (hexanes−ethyl acetate, 85:15, 2 mL/min, Spherisorb S5W 5μm); [α] = +36.0 (*c* = 0.0045, $CHCl_3$); ^{1}H NMR (300.13 MHz, $CDCl_3$) δ (ppm) 1.34 (s, 3H), 1.38 (s, 3H), 3.56 (s, 3H), 3.73 (dd, *J* = 5.3, 8.5 Hz, 1H), 4.04 (dd, *J* = 6.0, 8.6 Hz, 1H), 4.35 (m, 3H), 7.38−7.55 (m, 5H); ^{13}C NMR (75.47 MHz, $CDCl_3$) δ (ppm) 25.2, 26.4, 55.5, 66.0, 66.2, 72.9, 84.7 (*J* = 27.9 Hz), 109.9, 117.5, 121.3, 125.1, 127.3, 128.4, 129.7, 132.1, 166.4; UV λ_{max} 232 nm ($CHCl_3$); MS (EI) *m*/*z* 348 (M^+); HRMS (EI) $C_{16}H_{19}O_5F_3$ found 348.11843, calcd 348.11845, Δm 0.02 mu. Anal. Calcd for $C_{16}H_{19}O_5F_3$: C, 55.17; H, 5.5. Found: C, 55.43; H, 5.28.

D-α,β-Isopropylidenegliceryl (*S*)-(+)-2-methoxy-2-(trifluoromethyl)-2-phenylacetate ((*S*)-27): HPLC t_R = 11.64 min (hexanes−ethyl acetate, 85:15, 2 mL/min, Spherisorb S5W 5μm); [α] = −37.2 (*c* = 0.026, $CHCl_3$); ^{1}H NMR (300.13 MHz, $CDCl_3$) δ (ppm) 1.34 (s, 3H), 1.38 (s, 3H), 3.55 (s, 3H), 3.72 (m, 1H), 4.01 (m, 1H), 4.36 (m, 3H), 7.36−7.55 (m, 5H); ^{13}C NMR (75.47 MHz, $CDCl_3$) δ (ppm) 25.2, 26.4, 57.2, 65.0, 66.1, 72.8, 84. (*J* = 27.9 Hz), 109.8, 117.5, 121.3, 125.1, 127.3, 128.4, 129.7, 132.0, 166.3; UV λ_{max} 232 nm ($CHCl_3$); MS (EI) *m*/*z* 348 (M^+); HRMS (EI) $C_{16}H_{19}O_5F_3$ found 348.11844, calcd 348.11845, Δm 0.01 mu.

(−)-Methyl D-β-hydroxyisobutyrate (*R*)-(−)-2-methoxy-2-phenylacetate ((*R*)-28): HPLC t_R = 29.03 min (hexanes−ethyl acetate, 85:15, 2 mL/min, μ-porasil); [α] = −67.3 (*c* = 0.0485, $CHCl_3$); ^{1}H NMR (300.13 MHz, $CDCl_3$) δ (ppm) 1.07 (d, *J* = 7.2 Hz, 3H), 2.75 (m, 1H), 3.39 (s, 3H), 3.57 (s, 3H), 4.17 (dd, *J* = 5.7, 10.9 Hz, 1H), 4.28 (dd, *J* = 7.3, 10.8 Hz, 1H), 4.74 (s, 1H), 7.28−7.42 (m, 5H); ^{13}C NMR (75.47 MHz, $CDCl_3$) δ (ppm) 13.3, 38.7, 51.6, 57.1, 65.8, 82.2, 126.9, 128.4, 128.5, 136.0, 170.1, 173.6; UV λ_{max} 236 nm ($CHCl_3$); MS (EI) *m*/*z* 266 (M^+); HRMS (EI) $C_{14}H_{18}O_5$ found 266.11541, calcd 266.11542, Δm 0.01 mu. Anal. Calcd for $C_{14}H_{18}O_5$: C, 63.15; H, 6.81. Found: C, 63.43; H, 6.49.

(−)-Methyl D-β-hydroxyisobutyrate (*S*)-(+)-2-methoxy-2-phenylacetate ((*S*)-28): HPLC t_R = 19.9 min (hexanes−ethyl acetate, 85:15, 3 mL/min, μ-porasil); [α] = +30.5 (*c* = 0.0415, $CHCl_3$); ^{1}H NMR (300.13 MHz, $CDCl_3$) δ (ppm) 1.09 (d, *J* = 7.2 Hz, 3H), 2.71 (m, 1H), 3.39 (s, 3H), 3.53 (s, 3H), 4.23 (m, 2H), 4.74 (s, 1H), 7.30−7.42 (m, 5H); ^{13}C NMR (75.47 MHz, $CDCl_3$) δ (ppm) 13.5, 38.7, 51.6, 57.2, 65.8, 82.2, 127.0, 128.4, 128.6, 136.0, 170.2, 173.7; UV λ_{max} 236 nm ($CHCl_3$); MS (EI) *m*/*z* 266 (M^+); HRMS (EI) $C_{14}H_{18}O_5$ found 266.11543, calcd 266.11542, Δm −0.01 mu.

(−)-Methyl D-β-hydroxyisobutyrate (*R*)-(−)-2-methoxy-2-(trifluoromethyl)-2-phenylacetate ((*R*)-29): HPLC t_R = 16.10 min (hexanes−ethyl acetate, 85:15, 2 mL/min, Spherisorb S5W 5μm); [α] = +23.5 (*c* = 0.0165, $CHCl_3$); ^{1}H NMR (300.13 MHz, $CDCl_3$) δ (ppm) 1.21 (d, *J* = 7.2 Hz, 3H), 2.87 (m, 1H), 3.52 (s, 3H), 3.63 (s, 3H), 4.43 (m, 2H), 7.37−7.51 (m, 5H); ^{13}C NMR (75.47 MHz, $CDCl_3$) δ (ppm) 13.7, 38.7, 51.9, 55.4, 67.3, 84.5 (*J* = 27.9 Hz), 117.4, 121.3, 125.1, 127.3, 128.4, 129.6, 132.1, 166.3, 173.6; UV λ_{max} 232 nm ($CHCl_3$); MS (EI) *m*/*z* 334 (M^+); HRMS (EI) $C_{15}H_{17}O_5F_3$ found 334.10270, calcd 334.10280, Δm 0.10 mu. Anal. Calcd for $C_{15}H_{17}O_5F_3$: C, 53.89; H, 5.13. Found: C, 54.11; H, 5.45.

(−)-Methyl D-β-hydroxyisobutyrate (*S*)-(+)-2-methoxy-2-(trifluoromethyl)-2-phenylacetate ((*S*)-29): HPLC t_R = 15.81 min (hexanes−ethyl acetate, 85:15, 2 mL/min, Spherisorb S5W 5μm); [α] = −41.0 (*c* = 0.0305, $CHCl_3$); ^{1}H NMR (300.13 MHz, $CDCl_3$) δ (ppm) 1.20 (d, *J* = 7.2 Hz, 3H), 2.87 (m, 1H), 3.52 (s, 3H), 3.64 (s, 3H), 4.38 (dd, *J* = 5.6, 10.9 Hz, 1H), 4.49 (dd, *J* = 7.0, 10.8 Hz, 1H), 7.37−7.52 (m, 5H); ^{13}C NMR (75.47 MHz, $CDCl_3$) δ (ppm) 13.6, 38.7, 51.9, 55.3, 67.3, 84.6 (*J* = 27.9 Hz), 84.8, 117.5, 121.3, 125.1, 127.3, 128.4, 129.6, 132.0, 166.2, 173.5; UV λ_{max} 232 nm ($CHCl_3$); MS (EI) *m*/*z* 334 (M^+); HRMS (EI) $C_{15}H_{17}O_5F_3$ found 334.10235, calcd 334.10280, Δm 0.45 mu.

Acknowledgment. This work was financially supported by grants from the CICYT (MAR95-1-33-CO2-O2 and PM95-0135) and from the Xunta de Galicia (XUGA-20901B95 and XUGA-20910B96). S.K.L. acknowledges the Spanish Ministry for Education and Science for a postdoctoral research grant. M.J.F. thanks the Xunta de Galicia and Fundación "Gil Dávila" for a grant.

JA972550B